OPTIMAL CONTROL OF POSITIONING SYSTEM
WITH NON-LINEAR RATE-TYPE DRIVE

by

KOJI SASAKI

S.B. in Mechanical Engineering, Keio University
March, 1966

S.M. in Mechanical Engineering, Stanford University
January, 1968

SUBMITTED IN PARTIAL FULFILLMENT OF THE
REQUIREMENTS FOR THE DEGREE OF
MASTER OF SCIENCE
AND MECHANICAL ENGINEER
at the

MASSACHUSETTS INSTITUTE OF TECHNOLOGY

January, 1970

Signature of Author . . . . Signature redacted . . . .
Department of Mechanical Engineering

Certified by . . . . Signature redacted . . . . .
Thesis Supervisor

Accepted by . . . . Signature redacted . . . . . .
Chairman, Departmental Graduate Committee

OPTIMAL CONTROL OF POSITIONING SYSTEM
WITH NON-LINEAR RATE-TYPE DRIVE

by

KOJI SASAKI

Submitted to the Department
of Mechanical Engineering
on January 23, 1970
in partial fulfillment of the requirement
for the degree of Master of Science

ABSTRACT

The optimal control of the 3rd order positioning system with a saturated rate-type drive subject to a step input is investigated. Linear analysis is done assuming the performance index $PI = \int_0^T (e^2 + P^* u^2)\,dt$ which defines the optimality. The optimal system behaviors are evaluated and a bridge to the conventional control approach is developed. Stability of the non-linear system with the feedback gains which is optimal for a linear system, is investigated. A limit cycle criterion is developed by applying the single-valued describing function method for saturation non-linearity.

Thesis Supervisor: Dr. Herbert H. Richardson
Title: Professor of Mechanical Engineering

ACKNOWLEDGMENT

The author wishes to recognize and to thank his thesis supervisor, Professor Herbert H. Richardson, for his encouragement and insightful suggestions. The author also thanks Professors Michael Athans, Devendra P. Garg, Robert P. Rafuse, Daniel Whitney and David N. Wormley, and Mr. Ronald Rothchild for their suggestions. Mr. Richard S. Sidell is gratefully acknowledged not only for his consultation on the computers but also for his advice.

In addition the author wishes to thank Mr. Evodio Llevada for his drafting work, and Misses Ann Iversen and Emily Wise for their typewriting.

LIST OF CONTENTS

Chapter 1

INTRODUCTION

1.1 System Investigated

The position control of a simple mass driven by a rate-type motor through an undamped shaft (Fig. 1) is proposed. A piston-type fluidic motor is considered here as a typical rate-type drive. Analysis for rate-type servo has been developed [12, 13, 14]. Linearized system equation with saturation is given by

$$\frac{d}{dt}\begin{bmatrix} x \\ \dot{x} \\ \ddot{x} \end{bmatrix} = \begin{bmatrix} 0 & \omega_n & 0 \\ 0 & 0 & \omega_n \\ 0 & -\omega_n & -2\zeta_n\omega_n \end{bmatrix}\begin{bmatrix} x \\ \dot{x} \\ \ddot{x} \end{bmatrix} + \begin{bmatrix} 0 \\ 0 \\ k_v' \end{bmatrix} SAT(u) \tag{1-1}$$

$$y = [1 \ 0 \ 0]\begin{bmatrix} x \\ \dot{x} \\ \ddot{x} \end{bmatrix}$$

where x = non-dimensionalized position of mass

$\dot{x}$ = non-dimensionalized velocity of mass

$\ddot{x}$ = non-dimensionalized acceleration of mass

ω_n = natural frequency of open-loop system (rad/sec)

ζ_n = damping ratio in open-loop system

k_v' = non-dimensionalized open-loop gain

u = input to open-loop system

SAT(u) = saturation function defined by Equation (1-3)

t = time (sec)

y = output of system

When valves are fully open, there is no additional input to the ram even with more command signal to the valve. This is the saturation to be considered and is defined

$$\mathrm{SAT}\,(u) = \begin{cases} u & \text{for} \quad |u| \leq 1 \\ 1 & \text{for} \quad |u| > 1 \end{cases} \tag{1-2}$$

Input-output relation between u and x could be given by

$$X(s) = \frac{k_v'}{\frac{s}{\omega_n}\left(\frac{s^2}{\omega_n^2} + \frac{2\zeta}{\omega_n}s + 1\right)} \cdot SAT(U(s)) \tag{1-3}$$

where s = Laplace variable.

The modeling and mathematical formulation of this system is in Appendix I. A typical application could be azuma control of a radar antenna (Fig. 3, 4).

1.2 Objective of Study

The problem proposed is the optimal control of the position of the mass to a step input. The studies for the system with and without saturation are done for reasonably wide ranges of generalized system parameters.

For linear system, a bridge between modern optimal and conventional controls is developed.

1.3 Scope and Organization of Thesis

1.3.1 Outline of Problem and Study

Outline is listed below.

(1) Problem is optimal position control of 3rd-order system (Fig. 2, 5).

(2) Study is deterministic and classified as an Initial Condition Problem or a State Regulator Problem [3] which is developed for a step input only.

(3) All the states are fedback in both linear and non-linear studies (Fig. 6a, 14a).

(4) Linear Analysis is developed by considering that:

(a) Optimal criterion used is $PI = \int_0^T (e^2 + \overset{*}{p}u^2)\, dt$

(b) Optimal control law $u(x(t),t)$ is obtained by solving the matrix Riccati Equation or Hamilton-Jacobi Equation.

(c) A bridge (Fig. 12) to conventional control method should be developed; i.e., once a desired response is chosen for a given system from one of the charts about system response [Clark pp. 140-145], optimal feedback gains are immediately found by using Fig. 7, 8, and 12.

(d) Also system performance is evaluated and given in Fig. 11. The analytical study on the asymptotical behaviors of evaluated system performance curve shows that once a typical point is computed, the curve is ready to be drawn.

(e) Non-linear study is an extension of the linear study.

(a) The non-linearity is saturation at the motor valve (Fig. 1a) and characterized as in Fig. 15.

(b) Normalized step input size R_o to give saturation in control u is obtained (Fig. 18).

(c) Step input size R_o to give an unstable limit cycle is obtained both graphically by the single-valued describing function method and by direct digital simulations (Fig. 17 and 18).

1.3.2 Organization of Thesis

(1) Linear and non-linear analyses are given in Chapter 2.

(2) Overall conclusions and recommendations are given in Chapter 3.

(3) Modeling and mathematical formulation of the proposed physical system are given in Appendix I for interested readers.

(4) Computational Procedures for Analysis is given in Appendix II.

(5) Analytical solutions for the asymptotes of system-performance-evaluation plot are given in Appendix III.

Chapter 2

ANALYTICAL PROCEDURES AND RESULTS

2.1 Linear Analysis

2.1.1 Normalized Open-loop System

Modeling and mathematical formulation are done in Appendix I as mentioned in Chapter 1. In linear case, open-loop system has no saturation. By replacing SAT (u) in Eq. (1-1), open-loop system is given by

$$\frac{d}{dt}\begin{bmatrix} x \\ \dot{x} \\ \ddot{x} \end{bmatrix} = \begin{bmatrix} 0 & \omega_n & 0 \\ 0 & 0 & \omega_n \\ 0 & -\omega_n & -2\zeta_n\omega_n \end{bmatrix}\begin{bmatrix} x \\ \dot{x} \\ \ddot{x} \end{bmatrix} + \begin{bmatrix} 0 \\ 0 \\ k_v' \end{bmatrix} u \tag{2-1}$$

$$y = \begin{bmatrix} 1 & 0 & 0 \end{bmatrix}\begin{bmatrix} x \\ \dot{x} \\ \ddot{x} \end{bmatrix}$$

In order to non-dimensionalize the equation with respect to time, dimensionless time t' is defined by

$$t' = \omega_n t \tag{2-2}$$

By noting

$$\frac{d}{dt'} = \frac{1}{\omega_n}\frac{d}{dt} \tag{2-3}$$

and defining

$$k_v = \frac{k_v'}{\omega_n} \tag{2-4}$$

the open-loop system is written as

$$\frac{d}{dt'}\begin{bmatrix} x \\ \dot{x} \\ \ddot{x} \end{bmatrix} = \begin{bmatrix} 0 & 1 & 0 \\ 0 & 0 & 1 \\ 0 & -1 & -2\zeta_n \end{bmatrix}\begin{bmatrix} x \\ \dot{x} \\ \ddot{x} \end{bmatrix} + \begin{bmatrix} 0 \\ 0 \\ k_v \end{bmatrix} u \tag{2-5}$$

$$y = \begin{bmatrix} 1 & 0 & 0 \end{bmatrix}\begin{bmatrix} x \\ \dot{x} \\ \ddot{x} \end{bmatrix}$$

or

$$\frac{d}{dt'}\underline{x} = \underline{A}\,\underline{x} + \underline{b}\,u$$

$$y = \underline{c}\,\underline{x} \tag{2-6}$$

where

$$\underline{x} = \begin{bmatrix} x_1 \\ x_2 \\ x_3 \end{bmatrix} = \begin{bmatrix} x \\ \dot{x} \\ \ddot{x} \end{bmatrix}$$

The open-loop transfer function G(s) is given by

$$G(s') = \frac{X(s')}{U(s')} = \frac{k_v}{s'(s'^2 + 2\zeta_n s' + 1)} \tag{2-7}$$

where s' is Laplace variable corresponds to the dimensionless time variable t'.

In order to avoid complexity on variables, dimensionless t' and s' drop their dashes.

The open-loop system equation and its transfer function (between input u and state x) now rewritten as

$$\frac{d}{dt}\underline{x} = \underline{A}\,\underline{x} + \underline{b}\,u$$

$$y = \underline{c}\,\underline{x} \tag{2-8}$$

$$G(s) = \frac{X(s)}{U(s)} = \frac{k_v}{s(s^2 + 2\zeta_n s + 1)} \tag{2-9}$$

2.1.2 Closed-loop System (Control System) and Design Criteria

<u>System Configuration</u> (Fig, 6)

All the state variables should be fedback according to the Modern Control Theory. The system is in the form of Phase variables which contain all the necessary information to control it. The closed-loop system equation is given by

$$\frac{d}{dt}\underline{x} = \underline{A}_c\underline{x} + \underline{b}_c u$$
$$y = \underline{c}\,\underline{x}$$
$$u = r_o - \underline{K}^T\underline{x} \qquad (2\text{-}10)$$
$$\underline{x}(0) = \underline{0}$$

where r_o = step input to closed system applied at $t=0$

$\underline{K}$ = $[k_1, k_2, k_3]$ = feedback gain vector

Eq. (2-10) can be written as

$$\frac{d}{dt}\underline{x} = \begin{bmatrix} 0 & 1 & 0 \\ 0 & 0 & 1 \\ -k_1 & -(1+k_2) & -(2\xi_n+k_3) \end{bmatrix}\underline{x} + \begin{bmatrix} 0 \\ 0 \\ k_v \end{bmatrix} r_o \qquad (2\text{-}11)$$

$$\underline{x}(0) = \underline{0}$$

Closed-loop transfer function between r_o and x_1 is given by

$$G_c(s) = \frac{X_1(s)}{R_o(s)} = \frac{k_1 k_v}{s^3 + s^2(2\xi_n+k_3) + s(1+k_2) + k_1 k_v} \qquad (2\text{-}12)$$

Design Criteria Specified

(a) Zero steady-state error

(b) Stability of the system

(c) Possible minimum transient square error defined by Eq. (2-18). The error e is defined by

$$e = r_o - x_1 \qquad (2\text{-}13)$$

2.1.3 Zero Steady-State Error

From the closed-loop transfer function in Eq. (2-12),

$x_1(s)$ is given by

$$X_1(s) = G_c(s) \cdot \frac{R_o}{s} \tag{2-14}$$

where R_o = magnitude of step input $r_o(t)$ to the closed-loop system.

By applying the Final-value Theory,

$$\lim_{t \to \infty} x_1(t) = R_o = r_o(t > 0^+)$$

Since error e(t) is defined by Eq.(2-13), the steady-state error is zero.

2.1.4 Controllability and Observability

The closed-loop system is the 3rd-order single input-output system and from Eq. (2-11),

$$\underline{A}_c = \begin{bmatrix} 0 & 1 & 0 \\ 0 & 0 & 1 \\ -k_1 & -(1+k_2) & -(2\zeta_n+k_3) \end{bmatrix} \qquad \underline{b}_c = \begin{bmatrix} 0 \\ 0 \\ k_1 k_v \end{bmatrix} \tag{2-15}$$

<u>Controllability</u>

By the Controllability Theorem, the system is controllable because 3 x 3 composite matrix

$$\left[\, \underline{b}_c \;\; \underline{A}_c \underline{b}_c \;\; \underline{A}_c^2 \underline{b}_c \,\right] \tag{2-16}$$

is non-singular.

<u>Observability</u>

By the Observability Theorem, the system is observable because 3 x 3 composite matrix,

$$\left[\underline{C}^T \quad \underline{A}_c^T \underline{C}^T \quad (\underline{A}_c^T)^2 \underline{C}^T\right] \tag{2-17}$$

is non-singular.

2.1.5 Criterion of Optimality and Stability

Criterion of Optimality

Optimality of the system is desired to be defined as

$$\int_0^T e_{opt}^2(t)\,dt \le \int_0^T e^2(t)\,dt \tag{2-18}$$

where $e_{opt}(t)$ = error in optimal system

T = time gives the steady-state response

In order to solve the problem, a quadratic performance index PI is defined by

$$PI = \int_0^T \left[e^2(t) + p \cdot u^2(t)\right] dt \tag{2-19}$$

where P = weighting constant

Stability

General performance index in quadratic form is given by

$$PI = \int_0^\infty \left[\underline{x}^T \underline{Q}\, \underline{x} + \underline{u}^T \underline{P}\, \underline{u}\right] dt \tag{2-20}$$

Kalman (1964) has shown that in order to ensure stability, the pair $[\underline{A}, \underline{\Gamma}^T]$ must be completely observable, where $\underline{\Gamma}$ is defined by

$$\underline{Q} = \underline{\Gamma}\,\underline{\Gamma}^T \tag{2-21}$$

In this problem,

$$\underline{Q} = \begin{bmatrix} 1 & 0 & 0 \\ 0 & 0 & 0 \\ 0 & 0 & 0 \end{bmatrix} \qquad \underline{\Gamma} = \begin{bmatrix} 1 \\ 0 \\ 0 \end{bmatrix} \tag{2-22}$$

where $\underline{\Gamma}^T$ corresponds to $\underline{c}$ in Eq. (2-6).

Since

$$\left[\underline{\Gamma} \quad \underline{A}^T\underline{\Gamma} \quad (\underline{A}^T)^2\underline{\Gamma} \right] \tag{2-23}$$

is non-singular, the controlled linear system is stable with the performance index of Eq. (2-19).

2.1.6 Method to Find Optimal Control Law

Optimal Control Law

Optimal control law $u^\circ(\underline{x},t)$ for the open-loop system of Eq. (2-5) with the performance criterion $PI = \int_0^T (e^2 + \rho u^2)dt$ is given by

$$u^\circ(\underline{x},t) = -\rho^{-1}\,\underline{b}^T \underline{R_s}\,\underline{x} \tag{2-24}$$

or

$$u^\circ(\underline{x},t) = -\underline{k}^T\,\underline{x} \tag{2-25}$$

where $\underline{R_s}$ is the steady-state solution of the matrix Riccati equation,

$$\dot{\underline{R}}(t) + \underline{Q} - \underline{R}(t)\underline{b}\,\rho^{-1}\underline{b}^T\underline{R}(t) + \underline{R}(t)\underline{A} + \underline{A}^T\underline{R}(t) = 0 \tag{2-26}$$

A numerical solution for $\underline{R}(t)$ can be obtained on a digital computer, by integrating the Riccati equation backward in time from the known terminal condition over the time interval of interest [3]. The matrix $\underline{K}$ is referred to as the set of the optimal feedback gains or the coefficients.

Modification on $\underline{b}$ Matrix of Open-loop System

In order to reduce one of the parameters for simulation, $\underline{b}^*$ is defined as

$$\underline{b} = k_v \, \underline{b}^* = k_v \begin{bmatrix} 0 \\ 0 \\ 1 \end{bmatrix} \tag{2-27}$$

Eq. (2-26) can be rewritten as

$$\dot{\underline{R}}(t) + \underline{Q} - \frac{\underline{R}(t)\, k_v^2 \, \underline{b}^* \underline{b}^{*T} \underline{R}(t)}{p} + \underline{R}(t)\underline{A} + \underline{A}^T \underline{R}(t) = 0 \tag{2-28}$$

by also considering p is a scalar. By defining a new cost ratio P* as

$$\frac{1}{p^*} = \frac{k_v^2}{p} \tag{2-29}$$

Eq. (2-28) becomes,

$$\dot{\underline{R}}(t) + \underline{Q} - \frac{\underline{R}(t)\, \underline{b}^* \underline{b}^{*T} \underline{R}(t)}{p^*} + \underline{R}(t)\underline{A} + \underline{A}^T \underline{R}(t) = 0 \tag{2-30}$$

2.1.7 Control System to be Simulated

Now the optimal control problem is stated as a state-regulator problem of

$$\frac{d}{dt}\underline{x} = \underline{A}\,\underline{x} + \underline{b}^* u \tag{2-31a}$$

$$u = r_o - \underline{K}^T \underline{x} = r_o - \frac{\underline{b}^{*T} \underline{R}_s}{p^*} \underline{x} \tag{2-31b}$$

$$\underline{x}(0) = \underline{0} \tag{2-31c}$$

$$y = \underline{c}\, \underline{x} \tag{2-31d}$$

$$PI = \int_0^T (e^2 + p^* u^2)\, dt \tag{2-31e}$$

$$e = r_o - x_1 \tag{2-31f}$$

where

$$\underline{A} = \begin{bmatrix} 0 & 1 & 0 \\ 0 & 0 & 1 \\ 0 & -1 & -2\zeta_m \end{bmatrix} \qquad \underline{b}^* = \begin{bmatrix} 0 \\ 0 \\ 1 \end{bmatrix} \tag{2-31g}$$

$$\underline{c} = [\,1 \;\; 0 \;\; 0\,] \tag{2-31h}$$

$$x = \begin{bmatrix} x_1 \\ x_2 \\ x_3 \end{bmatrix} = \begin{bmatrix} x \\ \dot{x} \\ \ddot{x} \end{bmatrix} = \begin{bmatrix} \text{position of mass} \\ \text{velocity of mass} \\ \text{acceleration of mass} \end{bmatrix} \qquad (2\text{-}31i)$$

u = control

r_o = step input of magnitude R_o, applied at $t = 0$.

$\underline{K}$ = a set of optimal feedback gains

p^* = cost ratio

$\underline{R}_s$ = steady-state solution of

$$\dot{\underline{R}}(t) + \underline{Q} - \frac{\underline{R}(t)\,\underline{b}^*\underline{b}^{*T}\underline{R}(t)}{p^*} + \underline{R}(t)\,\underline{A} + \underline{A}^T\underline{R}(t) = 0 \qquad (2\text{-}31j)$$

y = output

PI = performance index

e = error

ζ_n = damping ratio in the open-loop system

The system is non-dimensionalized (Appendix I) and dimensionless time $\omega_n t$ is used (Eq. 2-2), where ω_n is the natural frequency of the open-loop system. This is the last form of the closed-loop system (control system) to be simulated. The configuration is given in Fig. 6a, where the transfer function G(s) between u and x_1 is given by

$$G(s) = \frac{X_1(s)}{U(s)} = \frac{1}{s(s^2 + 2\zeta_n s + 1)} \qquad (2\text{-}32)$$

The optimal closed-loop system transfer function $G_c(s)$, Eq. (2-12), should be rewritten as

$$G_c(s) = \frac{X_1(s)}{R_o(s)} = \frac{k_1}{s^3 + s^2(2\zeta_n + k_3) + s(1+k_2) + k_1} \qquad (2\text{-}33)$$

2.1.8 Simulation

Simulation

The word "simulation" is used here as an estimation of system behaviors on either digital or analog computer.

Computational Procedures

The diagram of computational procedures to obtain the results of interest is given in Fig. 19. The computer techniques used are briefly discussed in Appendix II.

2.1.9 Optimal Control System

The transfer function, Eq. (2-33), of the optimal control system can also be written as

$$G_c(s) = \frac{X_1(s)}{R_0(s)} = \frac{\alpha \omega_s^2}{(s+\alpha)(s^2 + 2\zeta_s \omega_s s + \omega_s^2)} \qquad (2\text{-}34)$$

where, as shown in Fig. 12,

α = real root of the optimal control system

ζ_s = damping ratio of the optimal control system

ω_s = frequency of the optimal control system

A system parameter β is defined by

$$\beta = \frac{\alpha}{\zeta_s \omega_s} \qquad (2\text{-}35)$$

The results of computation are given in Fig. 7 through Fig. 12.

The step response of the system is given by [1]

$$X_1(s) = \frac{R_0}{s} \cdot \frac{\alpha \omega_s^2}{(s+\alpha)(s^2 + 2\zeta_s \omega_s s + \omega_s^2)} \qquad (2\text{-}36)$$

or

$$x_1(t) = R_0\left[1 - \frac{\omega_s^2}{\alpha^2 - 2\zeta_s\omega_s\alpha + \omega_s^2} e^{-\alpha t} + \frac{\alpha\, e^{-\zeta_s\omega_s t} \sin(\omega_0 t + \psi)}{\sqrt{1-\zeta_s^2}\sqrt{\alpha^2 - 2\zeta_s\omega_s\alpha + \omega_s^2}}\right] \quad (2\text{-}37)$$

where

$$\omega_0 = \omega_s\sqrt{1-\zeta_s^2}$$

$$\theta = \tan^{-1}\left[\frac{\omega_0}{\alpha - \zeta_s\omega_s}\right]$$

$$\psi = \begin{cases} \tan^{-1}\dfrac{\sqrt{1-\zeta_s^2}}{\zeta_s} - \theta - \pi & \text{if } \theta \geq 0 \\ \tan^{-1}\dfrac{\sqrt{1-\zeta_s^2}}{\zeta_s} - \theta & \text{if } \theta < 0 \end{cases}$$

(1) Optimal Feedback Gains (Fig. 7)

Fig. 7 is the plot of $\underline{K}$ (vs. P^*) which is obtained by solving the matrix Riccati equation, Eq. (2-31j). $\underline{K}$ - P^* plot shows that:

(1a) k_1, k_2, k_3 increases monotonically as P^* decreases.

(1b) $\underline{K}$ is larger for the system whose ζ_n is larger.

(1c) $k_1 = \dfrac{1}{\sqrt{P^*}}$ for any ζ_n (2-38)

(1d) k_2 is almost identical for any ζ_n if $P^* < 10^{-1}$. For any ζ_n, the asymptote of k_2 as P^* approaches zero, is given by

$$k_2 \cong \frac{2}{(P^*)^{\frac{1}{3}}} \quad \text{if} \quad P^* < 10^{-2} \quad (2\text{-}39)$$

(1e) k_3 is almost identical for any ζ_n if $P^* < 10^{-6}$. Asymtote of k_3 as P^* goes to zero, for any ζ_n, is given by

$$k_3 \cong \frac{2}{(P^*)^{\frac{1}{6}}} \quad \text{if} \quad P^* < 10^{-6} \quad (2\text{-}40)$$

(1f) By knowing the relation between ζ_s and P* which is to be given by Fig. 8, Eq. (2-38) through Eq. (3-40) are rewritten as

$$k_1 \cong \omega_s^3 \tag{2-41}$$

$$k_2 \cong 2\omega_s^2 \qquad \text{if } P^* < 10^{-2} \tag{2-42}$$

$$k_3 \cong 2\omega_s \qquad \text{if } P^* < 10^{-6} \tag{2-43}$$

(2) Natural Frequency (Fig. 8)

Fig. 8 is the plot of ω_s (vs. P*) which is obtained by finding the roots of the characteristic equation of the system. (Eq. (2-33)). The plot shows that:

(2a) ω_s increases monotonically as P* approaches zero and ω_s's are almost identical for any ζ_n, if $P^* < 10^{-4}$. Approximation, for any ζ_n, can be as

$$\omega_s \cong \frac{1}{(P^*)^{\frac{1}{6}}} \qquad \text{if} \quad P^* < 10^{-4} \tag{2-44}$$

(2b) ω_s is larger for the system whose ζ_n is larger.

(3) Root Locus (Fig. 9)

The root locus of the system for each ζ_n, with P* as parameter, is plotted by knowing the characteristic roots of the system, Eq. (2-33). The root loci show that:

(3a) As ω_s goes larger (or P* approaches zero), the optimal system for any ζ_n becomes identical. This is true if $\omega_s \geq 4.6$ (or equivalently $P^* < 10^{-4}$).

(3b) For any ζ_n the optimal system approaches to have,

$$\zeta_s = 0.5 \tag{2-45}$$

$$\beta = 2.0 \tag{2-46}$$

(3c) The system is stable apparently.

(3d) For $\zeta_n = 1.0$, the optimal system has 3 real roots if $P^* > 6$.

(4) <u>A Typical Step Response</u> (Fig. 10)

The open-loop system in this example has $\zeta_n = 0$ with $P^* = 10^{-4}$ and $R_o = 0.008$. The resultant optimal system has

$$\underline{K} = \begin{bmatrix} 99.9 \\ 41.7 \\ 9.13 \end{bmatrix}$$

$$\zeta_s = 0.488 \qquad \omega_s = 4.68 \qquad \beta = 2.00$$

The plot shows that:

(4a)

$$|x_1(0^+)| \geq |x_1(t)| \qquad \text{for} \quad 0^+ \leq t \leq T \tag{2-47}$$

$$|u(0^+)| \geq |u(t)| \qquad \text{for} \quad 0^+ \leq t \leq T \tag{2-48}$$

(5) <u>Evaluation of Performance Index</u> (Fig. 11)

Evaluation of performance index for each optimal system to a unit step input is plotted as $\tilde{e}^2$ vs. $\tilde{u}^2$, with P^* as parameter,

where
$$\tilde{e}^2 = \int_0^T e^2 \, dt \tag{2-49}$$

$$\tilde{u}^2 = \int_0^T u^2 \, dt \tag{2-50}$$

The plot shows that:

(5a) $\tilde{e}^2$ decreases monotonically as $\tilde{u}^2$ increases, for any ζ_n

(5b) As ω_s goes larger (or P* approaches zero), $\tilde{e}^2$ decreases and $\tilde{u}^2$ increases.

(5c) For a fixed value of $\tilde{u}^2$, system with smaller ζ_n has smaller $\tilde{e}^2$.

(5d) For $P^* \leq 10^{-4}$ (or $\omega_s > 4.6$),

$$\omega_s \cong \frac{1}{(P^*)^{\frac{1}{6}}}$$

and

$$\tilde{e}^2 \cong \frac{5}{3}\frac{1}{\omega_s} \cong \frac{5}{3}(P^*)^{\frac{1}{6}} \tag{2-51}$$

$$\tilde{u}^2 \cong \frac{1}{3}\omega_s^5 \cong \frac{1}{3}(P^*)^{-\frac{5}{6}} \tag{2-52}$$

and so,

$$\tilde{e}^2 \cong \frac{5}{3}(3\tilde{u}^2)^{-\frac{1}{5}} \tag{2-53}$$

(5e) For $P^* \geq 10^4$ (or $\omega_s \cong 1.0$ for $\zeta_n \neq 0$)

$$\tilde{e}^2 \cong \frac{1}{2\alpha} \quad \left(\text{or} \quad = \frac{1}{2P_1} \quad \text{if } \zeta_n = 1.\right) \tag{2-54}$$

$$\tilde{u}^2 \cong \frac{\alpha}{2} \quad \left(\text{or} \quad = \frac{P_1}{2} \quad \text{if } \zeta_n = 1\right) \tag{2-55}$$

and so,

$$\tilde{e}^2 \cong \frac{1}{4\tilde{u}^2} \tag{2-56}$$

In Appendix III, the results (5d) and (5e) are obtained analytically.

(6) <u>A Bridge to a Conventional Control</u> (Fig. 12)

The plot is ζ_s vs. β for $\zeta_n = 0 \sim 1.0$ with P* as parameter. It shows that:

(6a) The optimal system for any ζ_n,

$$\beta \cong 2 \qquad \text{for} \quad P^* < 10^{-4} \tag{2-57}$$

$$\zeta_s \cong 0.5 \qquad \text{for} \quad P^* < 10^{-4} \tag{2-58}$$

(6b) Once designer specifies ζ_s and β about given open-loop system (fixed ζ_n), Fig. 12 tells proper P* with which optimal feedback gains are obtained.

2.1.10 Conclusions

Conclusions are made from the results simulated on the control system stated by Eq. (2-31a) through (2-31j). The design criteria specified in 2.1.2 are repeated here for convenience; i.e.,

(a) Zero steady-state error

(b) Stability of the system

(c) Possible minimum transient square error defined by

$$\int_0^T e_{opt}^2(t)\,dt \le \int_0^T e^2(t)\,dt \qquad \text{(Eq. (2-18))}$$

<u>Conclusion (1)</u> Optimal System defined with the performance index criterion ($PI = \int_0^T (e^2 + P^* u^2)dt$) approaches the minimum square error system ($\int_0^T e_{opt}^2\,dt \le \int_0^T e^2\,dt$) as P* becomes small. Actually, Fig. 12 shows that for an open-loop system with any ζ_n, the resultant optimal closed-loop system becomes identical and its system characteristics are given by

$$\zeta_s = 0.5 \qquad \text{(Eq.(2-45))}$$

$$\beta = 2.0 \qquad \text{(Eq.(2-46))}$$

if $\quad P^* < 10^{-4}$

where ω_s can be well approximated by Eq. (2-44) as

$$\omega_s \cong \frac{1}{(P^*)^{\frac{1}{6}}}$$

The condition $P^* < 10^{-4}$, therefore, can be replaced by

$$\omega_s \geq 4.6 \text{ (rad)}$$

or

$$\frac{\omega_s}{\omega_n} > 4.6 \text{ (sec)}$$

which may be referred to Eq. (2-2).

The reason why the closed-loop system can have $\zeta_s \cong 0.5$ and $\beta \cong 2.0$ only if $P^* < 10^{-4}$ is that the permissible amount of control u for shifting the poles of the original open-loop system to the optimal location, is limited unless P^* is small enough. The result, in Fig. 11 ($\tilde{e}^2$-$\tilde{u}^2$), which shows that at $P^* = 1$,

$$\tilde{e}^2_{\zeta_n=0} < \tilde{e}^2_{\zeta_n=0.5} < \tilde{e}^2_{\zeta_n=1.0}$$

$$\tilde{u}^2_{\zeta_n=0} < \tilde{u}^2_{\zeta_n=0.5} < \tilde{u}^2_{\zeta_n=1.0}$$

is explained by the same reason; i.e., a large control u is required to shift heavily damped system's poles compared to slightly damped case.

Conclusion (2) From the Conclusion (1) optimal control system satisfies the design criteria specified only if $P^* < 10^{-4}$.

Naturally, the closed-loop system is optimal in the sense of

$$PI_{opt} \leq PI \qquad \text{for any } P^*$$

but not in the sense of

$$\int_0^T e_{opt}^2(t)\,dt \le \int_0^T e^2(t)\,dt$$

unless $P^* < 10^{-4}$.

Conclusion (3) $\underline{K}$ can be approximated by

$$k_1 = \omega_s^3 \tag{2-59}$$

$$k_2 = 2\omega_s^2 - 1 \qquad \text{if} \quad P^* < 10^{-2} \tag{2-60}$$

$$k_3 = 2\omega_s - 2\zeta_n \qquad \text{if} \quad P^* < 10^{-6} \tag{2-61}$$

These equations are simply obtained by equating Eq. (2-33) and Eq. (2-34) and by noticing

$\beta \cong 2.0$

$\zeta_s \cong 0.5$

for the optimal system with $P^* < 10^{-4}$. This is the identical result as when the Butterworth Polynomials Method is used.

Conclusion (4) Estimations of $|e|_{max}$ and $|u|_{max}$ for the optimal system can be easily made.

From Fig. 6a,

$$u(t) = k_1 e(t) - k_2 x_2(t) - k_3 x_3(t) \tag{2-62}$$

It is clear that

$$|e(0^+)| \ge |e(t)| \qquad 0^+ \le t \le T \tag{2-63}$$

$$|u(0^+)| \ge |u(t)| \qquad 0^+ \le t \le T \tag{2-64}$$

and

$$e(0^+) = R_o \tag{2-65}$$

provided the system is stable. Therefore,

$$|u|_{max} = k_1 |e|_{max} \tag{2-66}$$

where

$$|e|_{max} = |e(0^+)| = R_o \tag{2-67}$$

and

$$|u|_{max} = |u(0^+)| = k_1 R_o \tag{2-68}$$

$e(t)$ and $u(t)$ are linearly dependent on R_o (step input size) as

$$\left.\begin{array}{l} e(t) \rightarrow c\, e(t) \\ u(t) \rightarrow c\, u(t) \end{array}\right\} \text{ as } \quad R_o \rightarrow c\, R_o \tag{2-69}$$

where C is a constant. Since the step size R_o which gives $|u|_{max} = 1.0$ is shown (for each ζ_n) in Fig. 18 by a line named "saturation", $|e|_{max}$ and $|u|_{max}$ for any step input size of interest can be easily estimated by using Eq. (2-67) through Eq. (2-69), provided k_1 is known. The $|e|_{max}$ and $|u|_{max}$ can also be evaluated by directly computing Eq. (2-37).

<u>Conclusion(5)</u> Method to evaluate $\tilde{e}^2$ and $\tilde{u}^2$ is developed (Fig. 11). From result (5d), $\tilde{e}^2$ is given by Eq. (2-51) as

$$\tilde{e}^2 \cong \frac{5}{3} \frac{1}{\omega_s} \qquad \omega_s > 4.6$$

where ω_s is approximated by Eq. (2-44) as

$$\omega_s \cong \frac{1}{(p^*)^{\frac{1}{6}}} \qquad p^* < 10^{-4}$$

and the asymptote as ω_s goes larger is given by Eq. (2-53) as

$$\tilde{e}^2 \cong \frac{5}{3}(3\tilde{u}^2)^{-\frac{1}{5}} \qquad \omega_s > 4.6 \text{ (rad)}$$

From result (5e), $\tilde{e}^2$ is given by Eq. (2-54) as

$$\tilde{e}^2 \cong \frac{1}{2\alpha} \qquad P^* \geq 10^4 \quad , \zeta_n \neq 0$$

and the asymptote as P* approaches zero is given by Eq. (2-56) as

$$\tilde{e}^2 \cong \frac{1}{4\tilde{u}^2} \qquad P^* \geq 10^4 , \ \zeta_n \neq 0$$

Therefore, after knowing these asymptotes, the region of P* left to be investigated to evaluate its corresponding $\tilde{e}^2$ and $\tilde{u}^2$ is

$$10^4 < P^* < 10^{-4} \tag{2-70}$$

However, once one point in the middle of the region is evaluated, a rough plotting can be made by using the asymptotes. The above results are obtained only for step input size $R_o = 1$. For any size of R_o, the corresponding $\tilde{e}^2$ and $\tilde{u}^2$ are easily obtained by knowing

$$\left.\begin{array}{l} \tilde{e}^2 \rightarrow c^2\,\tilde{e}^2 \\ \tilde{u}^2 \rightarrow c^2\,\tilde{u}^2 \end{array}\right\} \text{ as } \quad R_o \rightarrow C R_o \tag{2-71}$$

where C is a constant.

Conclusion (6) A bridge between modern (optimal) and conventional controls is developed (Fig. 13).

Suppose ζ_n is specified in the given open-loop system. R_o (size of step input) is given. The desired ζ_s and β are specified by referring to step response charts in conventional control literatures [Clark pp. 140-145]. At this stage the combination of ζ_s and β must satisfy the curve given in Fig. 12 for ζ_n specified. Then, by the procedure shown in Fig. 13, the optimal closed-loop system ($\underline{K}$) and the estimations of its behaviors, ($|e|_{max}$, $|u|_{max}$, $\tilde{e}^2$ and $\tilde{u}^2$) are ready to be obtained, provided ω_s (or equivalently P*) is properly chosen. The resultant closed-loop system is the realization of the system specifications ζ_s and β. If the minimum error cost system ($\int_0^T e_{opt}^2\, dt \leq \int_0^T e^2\, dt$) is required, then the specifications must be $\zeta_s = 0.5$ and $\beta = 2.0$. Now ω_s must be larger than 4.6 (or equivalently $P^* < 10^{-4}$) and ω_s should be chosen by considering the values of $\tilde{e}^2$ and $\tilde{u}^2$ which are estimated by using Fig. 11 and Eq. (2-71).

2.2 Non-linear Analysis

2.2.1 Non-linear Open-loop System

Configuration

The open-loop system to be controlled consists of a non-linear element and the linear open-loop transfer function (Fig. 5). The linear open-loop system is the same as that in the linear analysis and its transfer function G(s) between $X_1(s)$ and $U_{sat}(s)$ (instead of $X_1(s)$ and $U(s)$) is given by

$$G(s) = \frac{X_1(s)}{U_{SAT}(s)} = \frac{1}{s(s^2 + 2\zeta_n s + 1)} \qquad (2\text{-}72)$$

The input-output relation of the non-linear open-loop system is given by

$$X_1(s) = \frac{1}{s(s^2 + 2\zeta_n s + 1)} \cdot \mathrm{SAT}(U(s)) \qquad (2\text{-}73)$$

Saturation in Physical Model

The saturation concerned here is one of the non-linearities that the physical system has. The saturation is one of the valve characteristics in the fluidic motor used. Suppose the valve is closed. Assume that the pressure drop between the ram chambers increases linearly as the valve opens until it opens fully. Once the valve opens fully, no additional **flow is** available, regardless of the command input to the valve increases.

Definition of SAT(u)

The mathematical model of the saturation is given by

$$u_{SAT} = SAT(u) = \begin{cases} u & \text{if } |u|<1 \\ 1 & \text{if } |u|\geq 1 \end{cases} \qquad (2\text{-}74)$$

This is shown in Fig. 15, where u and u_{SAT} are the input and the output to the saturation element respectively.

2.2.2 Non-linear Closed-loop System

System Configuration (Fig. 14a)

The control system configuration is identical to the linear case except the saturation element. All the state variables (phase variables) are fedback through the $\underline{K}$ obtained for the linear optimal control system.

System Equations

The control problem is again a state-regulator problem and the control system is given by

$$\frac{d}{dt}\underline{x} = \underline{A}\underline{x} + \underline{b}^* \, SAT(u) \qquad (2\text{-}75a)$$

$$SAT(u) = \begin{cases} u & \text{if } |u| < 1 \\ 1 & \text{if } |u| \geq 1 \end{cases} \tag{2-75b}$$

$$u = r_0 - \underline{K}^T \underline{x} \tag{2-75c}$$

$$\underline{x}(0) = \underline{0} \tag{2-75d}$$

$$y = \underline{c}\,\underline{x} \tag{2-75e}$$

$$e = r_0 - x_1 \tag{2-75f}$$

where

$$\underline{A} = \begin{bmatrix} 0 & 1 & 0 \\ 0 & 0 & 1 \\ 0 & -1 & -2\zeta_n \end{bmatrix} \qquad \underline{b}^* = \begin{bmatrix} 0 \\ 0 \\ 1 \end{bmatrix} \tag{2-75g}$$

$$\underline{c} = [1 \quad 0 \quad 0] \tag{2-75h}$$

$$\underline{x} = \begin{bmatrix} x_1 \\ x_2 \\ x_3 \end{bmatrix} = \begin{bmatrix} x \\ \dot{x} \\ \ddot{x} \end{bmatrix} = \begin{Bmatrix} \text{position of mass} \\ \text{velocity of mass} \\ \text{acceleration of mass} \end{Bmatrix} \tag{2-75i}$$

u = control

r_o = step-input of magnitude R_o, applied at T = 0

$\underline{K}$ = a set of optimal feedback gains obtained by solving the linear optimal control problem defined by Eq.'s (2-31a) through (2-31j), where the performance criterion is defined by Eq. (2-31e) as

$$PI = \int_0^T (e^2 + P^* u^2)\, dt$$

P* = cost ratio

y = output

e = error

ζ_n = damping ratio in the given open-loop system

2.2.3 Control System Behaviors

The only structural difference between the linear and the non-linear control systems is the saturation element. However, this gives important differences between their system behaviors.

Saturation and Optimality

The optimal feedback gains K for the linear control system are used for the non-linear control system, where these feedback gains are not optimal any more because of the saturation if the control u saturates. However, if the control u does not saturate too much or too often, the control system can be considered an approximately optimal system. Because the optimal control feedback gains depend upon the size of step-input in a much saturating case, the control system is called sub-optimal.

Limit Cycle and Stability

The characteristics of the saturation (Fig. 15) may cause limit cycles depending upon the size of step-inputs [9]. There may exist two kinds of limit cycles, stable and unstable (Fig. 17). However, the limit cycle of interest here is the unstable one which occurs with smaller step-input size than for the stable one, if any.

2.2.4 Simulation

Normalization of Step-input Size to Saturation Level

As mentioned in Saturation and Optimality of the previous section, the relative size of a step-input to the saturation level is essential. For this reason, the characteristics of the saturation is defined by Eq. (2-74) where it has the unit slope and the unit saturation levels (Fig. 15). Therefore, any size of a step-input is considered as normalized to the saturation levels.

Purpose of Simulation

From the linear analysis and Eq. (2-76), it is ready to obtain the minimum R_o which makes the control u saturate.

The purpose of simulation here is to obtain the minimum R_o which makes the system unstable with a limit cycle. There are two methods for it. First an approximate solution is obtained graphically with a single-valued describing function for the saturation [9]. Then, by using this result as a reference, the exact solution is found by a direct simulation.

When Non-linear System Behaves as Linear System

If control u is small enough so that it never saturates, then the non-linear control system is actually the linear control system and it is optimal, provided the non-linear system has the optimal feedback gains obtained for the linear system. This happens if

$$k_1 R_o \leq 1. \tag{2-76}$$

which should be clear from the Conclusion (4) of the linear analysis.

2.2.5 Limit Cycle Determination by Describing Function Method

The system (Fig. 14b) is equivalent to the closed-loop system (Fig. 14a). In Fig. 14b the input and the initial conditions are defined by

$$\left.\begin{aligned} r_0 &= 0 \\ x_1(0) &= -R_0 \\ x_2(0) &= x_3(0) = 0 \end{aligned}\right\} \qquad (2-77)$$

The characteristic equation of this system is

$$1 + G_d \, G \cdot H_{eq} = 0 \qquad (2-78)$$

where $G_d(R_o)$ = a single-valued describing function of the saturation.

$$G_d(R_0) = \frac{2}{\pi}\left[\sin^{-1}\left(\frac{1}{R_0}\right) + \left(\frac{1}{R_0}\right)\sqrt{1-\left(\frac{1}{R_0}\right)^2}\right] \qquad (2-79)$$

$$\left.\begin{aligned} G(s) &= \frac{1}{s(s^2 + 2\zeta_n s + 1)} \\ H_{eq}(s) &= k_3 s^2 + k_2 s + k_1 \end{aligned}\right. \qquad (2-80)$$

On the Nyquist plane, the characteristic equation is realized by the crossing point (s) between the 2 curves defined by

$$-\frac{1}{G_d(R_0)} \qquad 0 \le R_0 \le \infty \qquad (2-81)$$

and

$$G(j\omega_s)\,H_{eq}(j\omega_s) \qquad 0 < \omega_s \le \infty \qquad (2-82)$$

These 2 points give the stable and the unstable limit cycles for the specified closed-loop system (Fig. 14a). The existence of crossing points depends upon R_o as well as $G H_{eq}$ (Fig. 16).

2.2.6 Results

(1) R_{sat} = minimum step-input size R_o which makes control u saturate (Fig. 18).

Equation (2-76) with the value of k_1 obtained in the linear analysis gives the minimum R_o which makes u saturate.

(1a) R_{sat} increases monotonically as ω_s approaches unity (or equivalently as P* approaches infinity) for any ζ_n.

(1b) System with larger ζ_n has larger R_{sat} at a fixed ω_s (or P*).

(1c) R_{sat} is approximately identical for any ζ_n if $\omega_s > 4.6$ (rad) (or equivalently if $P^* < 10^{-4}$)

(1d) As ω_s increases, $R_{sat} - \omega_s$ plot approaches an asymptote characterized by

$$R_{SAT} = \frac{1}{\omega_s^3} \cong \sqrt{P^*} \tag{2-83}$$

(1e) As ω_s approaches unity, $R_{sa} - \omega_s$ plot approaches an asymptote characterized by

$$R_{SAT} \cong \frac{1}{\sqrt{P^*}} \tag{2-84}$$

(2) $R_{lim,\ approx.}$ = Approximate solution obtained by describing function method. The minimum R_o which makes system unstable with a limit cycle. (Fig. 18).

(2a) $R_{lim,\ approx.}$ increases monotonically as ω_s approaches unity (or equivalently as P* approaches infinity) for any ζ_n.

(2b) System with larger ζ_n has larger $R_{lim,\ approx.}$ at same ω_s (or P*).

(2c) As ω_s increases, $R_{lim,\ approx.} - \omega_s$ plot approaches an asymptote characterized by

$$R_{lim,approx.} \cong \frac{2}{\omega_s^3} \cong 2\sqrt{P^*} \tag{2-85}$$

(2d) No limit cycle exists with any ζ_n for $P^* \geq 1$.

(2e) No limit cycle exists with $\zeta_n = 0.5$ for $P^* \geq 10^{-2}$.

(2f) No limit cycle exists with $\zeta_n = 1.0$ for $P^* \geq 10^{-4}$.

(3) $R_{lim,\ sim}$ = simulated result. The minimum R_o which makes the system unstable with a limit cycle (Fig. 18).

(3a) Simulations are made for $P^* = 10^{-4}$ and $P^* = 10^{-6}$ with $\zeta_n = 0$ and $\zeta_n = 0.5$.

(3b) $R_{lim,\ sim}$ increases monotonically as ω_s decreases (or equivalently as P^* increases).

(3c) System with $\zeta_n = 0.5$ has larger $R_{lim,\ sim}$ than with $\zeta_n=0$ at a fixed ω_s (or P^*).

(4) Comparison between $R_{lim,\ sim}$ and $R_{lim,\ approx.}$

(4a) $R_{lim,\ approx}$ is smaller than $R_{lim,\ sim.}$

2.2.7 Conclusions

The definitions of R_{sat}, $R_{lim,\ approx.}$ and $R_{lim,sim}$ are re-stated here for convenience.

R_{sat} = minimum step-input size R_o which makes control u saturate.

$R_{lim,\ approx.}$ = approximate solution obtained by using describing function method. The minimum R_o which makes system unstable with a limit cycle.

$R_{lim,\ sim}$ = simulated result. The minimum R_o which makes system unstable with a limit cycle.

Conclusion (1) Qualitatively speaking, the system with smaller ζ_n is easier to have saturation in control u with same P^*.

Conclusion (2) For a fixed ζ_n, the system is easier to have saturation in control u when P* is smaller (or ω_s is larger).

Conclusion (3) For $P^* < 10^{-4}$, R_{sat} becomes approximately identical for any ζ_n and $R_{sat} - \omega_s$ plot approaches an asymptote defined by Eq. (2-83) as

$$R_{sat} = \sqrt{P^*}$$

which can be written by Eq. (2-83) as

$$R_{sat} \cong \frac{1}{\omega_s^3}$$

from the Conclusion (1) of the linear analysis.

Conclusion (4) For $P^* > 10^4$, R_{sat} becomes approximately identical for any ζ_n (except $\zeta_n = 1.0$) and $R_{sat} - \omega_s$ plot approaches an asymptote defined by Eq. (2-84) as

$$R_{sat} \cong \frac{1}{\sqrt{P^*}}$$

Conclusion (5) The system with smaller ζ_n is easier to have a limit cycle with a fixed P*.

Conclusion (6) For a fixed ζ_n, the system is easier to have a limit cycle when P* is smaller (or ω_s is larger).

Conclusion (7) With $P^* > 1$, system never has a limit cycle for any ζ_n.

Conclusion (8) $R_{lim,\ approx.} - \omega_s$ plot implies that it approaches an asymptote approximated by Eq. (2-85) as

$$R_{lim,\ approx} \cong 2\sqrt{P^*} \qquad \text{for } P^* < 10^{-4}$$

which can be rewritten by

$$R_{lim,\,approx} \cong \frac{2}{\omega_s^3} \qquad \text{for} \quad \omega_s > 4.6 \text{ (rad)} \qquad (2\text{-}86)$$

from the Conclusion (1) of the linear analysis.

Conclusion (9) The criterion for existence of a limit cycle by using describing function is conservative; i.e., even if this approximation method shows the existence of a limit cycle, there may not exist any. It is not accurate to state how it is conservative compared to the simulation, because of limited numbers of data.

CHAPTER 3

CONCLUSIONS AND RECOMMENDATIONS

3.1 System Studied

The linear and the non-linear systems investigated are defined by Eq.'s (2-31) and (2-75) respectively. Their configurations are given in Fig.'s 6a and 14a. The only difference between them is the saturation which is defined by Eq. (2-74). The time t in these non-dimensionalized equations is defined by Eq. (2-2) as

$$t = \omega_n \times (\text{dimentional time}) \ (\text{rad})$$

where ω_n = natural frequency of system to be controlled (rad/sec)

3.2 Conclusions

C1. An open-loop system with smaller ζ_n has a smaller ζ_s in its closed-loop system constructed by applying the optimal control theory with $PI = \int_0^T (e^2 + p^* u^2)\, dt$, because u is finite with finite P* (P* $\neq$ 0).

C2.
$$|e_1(t)|_{max} = |e_1(0^+)| = R_0$$

$$|u(t)|_{max} = |u(0^+)| = k_1 R_0 \qquad \text{(Eq. (2-67) and (2-68))}$$

(from Conclusion (4) of the linear analysis)

C3. For the linear systems,

$$\tilde{e}^2_{\zeta_n=0} \leq \tilde{e}^2 \leq \tilde{e}^2_{\zeta_n=1.0}$$

$$\tilde{u}^2_{\zeta_n=0} \leq \tilde{u}^2 \leq \tilde{u}^2_{\zeta_n=1.0}$$

with fixed P* and R_o. (From Conclusion (1) of the linear analysis.)

C4. For the linear system, the optimal feedback gains $\underline{K}$ obtained with

$$PI = \int_0^T (e^2 + p^* u^2)\, dt \qquad \text{(Eq. (2-31e))}$$

approximately satisfy

$$\int_0^T e_{opt}^2\, dt \leq \int_0^T e^2\, dt \qquad \text{(Eq. (2-18))}$$

(from Conclusion (2) of the linear analysis) where ω_s is approximated by

$$\omega_s \cong \frac{1}{(P^*)^{\frac{1}{6}}} \qquad \text{(Eq.(2-44))}$$

(from Conclusion (1) of the linear analysis)

and the optimal control system has

$$\zeta_s \cong 0.5 \qquad \text{(Eq.(2-45))}$$

$$\beta \cong 2.0 \qquad \text{(Eq.(2-46))}$$

(from Conclusion (1) of the linear analysis.

C5. For the linear system,

$$\left.\begin{aligned} \tilde{e}^2 &\rightarrow c^2\,\tilde{e}^2 \\ \tilde{u}^2 &\rightarrow c^2\,\tilde{u}^2 \end{aligned}\right\} \text{ as } R_0 \rightarrow c R_0 \qquad \text{(Eq.(2-71))}$$

(from Conclusion (5) of the linear analysis)

C6. For the linear system, $\tilde{e}^2 - \tilde{u}^2$ plot (Fig. 11) has the asymptotes defined by

$$\tilde{e}^2 \cong \frac{1}{4\tilde{u}^2} \qquad \text{for } P^* > 10^4 \qquad \text{(Eq.(2-56))}$$

$$\tilde{e}^2 \cong \frac{5}{3}(3\,\tilde{u}^2)^{-\frac{1}{5}} \qquad \text{for } P^* < 10^{-4} \qquad \text{(Eq.(2-53))}$$

(from Conclusion (5) of the linear analysis)

C7. A bridge between the modern (optimal) and the conventional controls is developed. Once the desired system response is specified, the optimal feedback gains $\underline{K}$ for the linear system are immediately obtained. (Fig. 12). (from Conclusion (6) of the linear analysis.

C8. For a specified R_o, the minimum P* which ensures no saturation is given by

$$P^* \geq R_o^2 \qquad \text{if} \quad P^* \leq 10^{-4} \qquad (3\text{-}1)$$

(from Eq. (2-83). If $P^* > 10^{-4}$, the $R_{sat} - \omega_s$ plot (Fig. 18) should be referred. (From Conclusion (3) of the non-linear analysis).

If P* is specified, the maximum R_o which ensures no saturation is given by

$$R_o \leq \sqrt{P^*} \qquad \text{if} \quad P^* \leq 10^{-4} \qquad (3\text{-}2)$$

(from Eq. (2-83). If $P^* > 10^{-4}$, the $R_{sat} - \omega_s$ plot (Fig. 18) should be referred. (From Conclusion (3) of the non-linear analysis).

C9. For a fixed ζ_n, the system with larger ω_s (or smaller P*) is easier to have the saturation in u and a limit cycle (if any), because it has the larger feedback gains $\underline{K}$. (From Conclusion (2) of the non-linear analysis.)

C10. The criterion with the describing function which determines the existence of a limit cycle is conservative compared to the direct simulation. (From Conclusion (9) of the non-linear analysis).

C11. For a fixed value of P*, the system with smaller ζ_n is easier to have the saturation in u and a limit cycle (if any), because smaller ζ_n corresponds smaller ζ_s as mentioned in C1. (From Conclusion (5) of the non-linear analysis.)

C12. $R_{sat} - \omega_s$ plot approaches an asymptote defined by

$$R_{sat} = \frac{1}{\omega_s^3} \quad \text{if} \quad P^* < 10^{-4} \qquad \text{(Eq. (2-83))}$$

(From Conclusion (3) of the non-linear analysis).

C13. $R_{lim,\ approx.} - \omega_s$ plot (for $\zeta_n = 0$) approaches an asymptote characterized by

$$R_{lim,\ approx} \simeq \frac{2}{\omega_s^3} \quad \text{if} \quad P^* < 10^{-4} \qquad \text{(Eq. (2-86))}$$

(From Conclusion (8) of the non-linear analysis.)

C14. By considering C9 through C13, a stability criterion is defined by

$$\frac{R_{lim,\ approx.}}{R_{sat}} \leq 2. \qquad \text{for any } P^* \text{ and } \zeta_n \qquad (3\text{-}3)$$

where

$$R_{sat} \simeq \frac{1}{\omega_s^3} \quad \text{if} \quad P^* < 10^{-4} \quad \text{from C12.}$$

(From Conclusion (8) of the non-linear analysis). This criterion says that no limit cycle exists for

$$R_o \leq 2\ R_{sat} \qquad (3\text{-}4)$$

3.3 Recommendations

R1. $R_{lim,sim} - \omega_s$ plot should be completed by referring to the $R_{lim,\ approx.} - \omega_s$ plot done. This could be done by developing a simulation program on a digital computer.

R2. $\tilde{e}^2 - \tilde{u}^2$ plot for R_o such that

$$R_{sat} < R_o < R_{lim,sim}$$

should be made so that the effect of increasing R_o on $\tilde{e}^2 - \tilde{u}^2$ could be studied.

R3. Once R2 was done, the behavior of a slightly saturating system (which may be considered as an almost optimal system) could be estimated.

LIST OF FIGURES

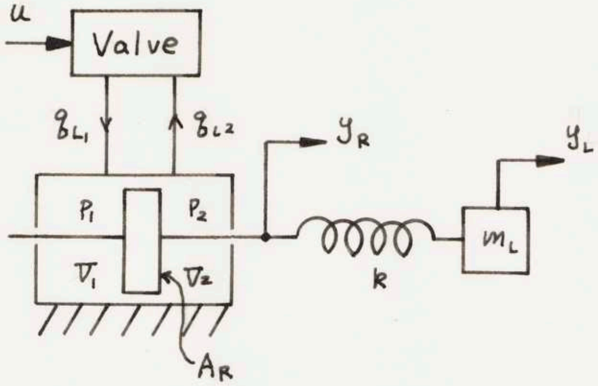

Fig. 1a. Open-loop Positioning System

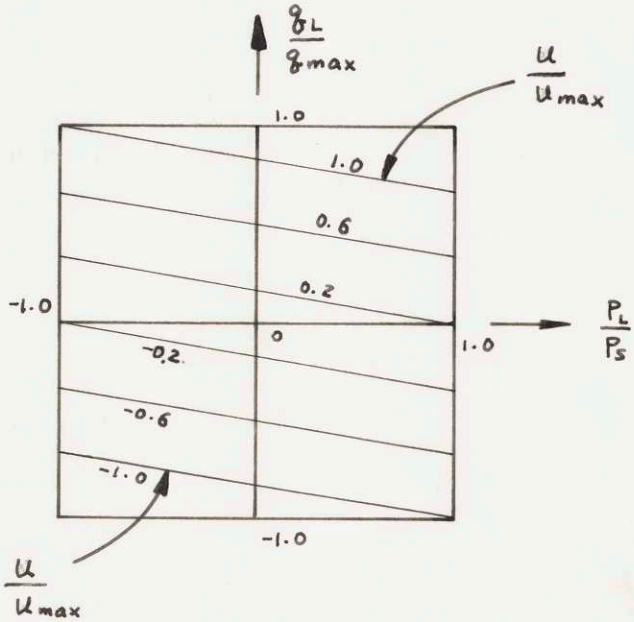

Fig. 1b. Linearized Pressure-Flow Characteristics of Underlapped Valve

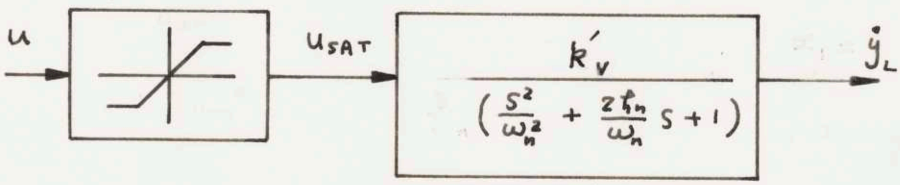

Fig. 2. Open-loop Positioning System

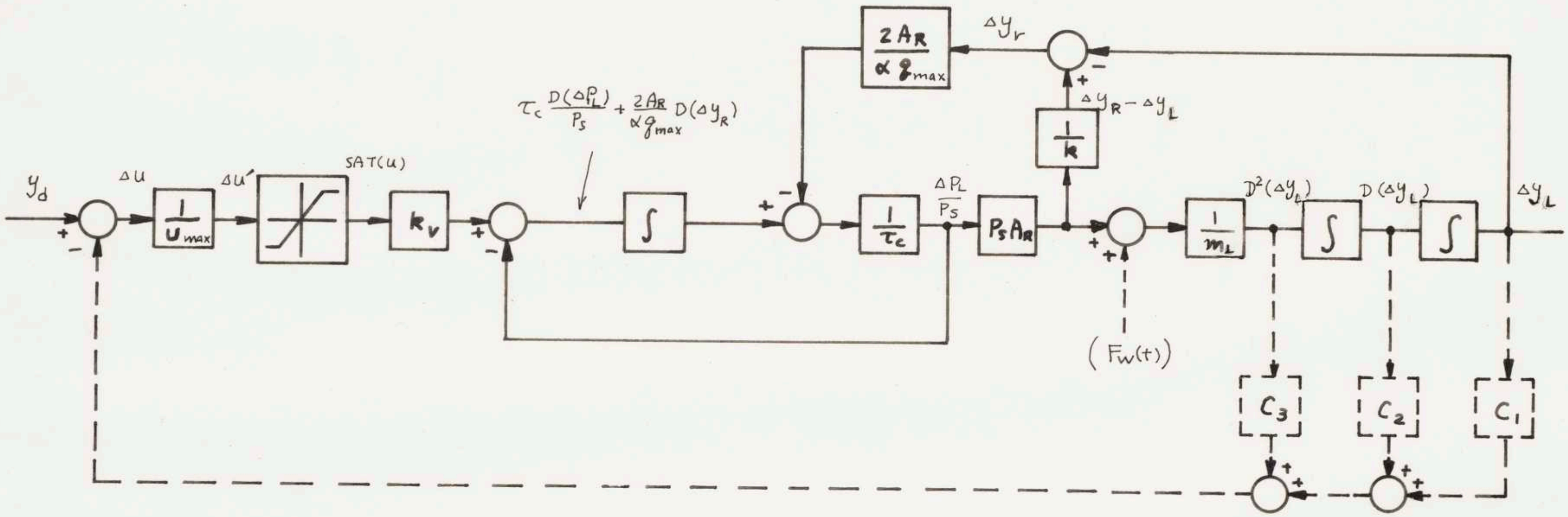

Fig. 1c. Open-loop Positioning System

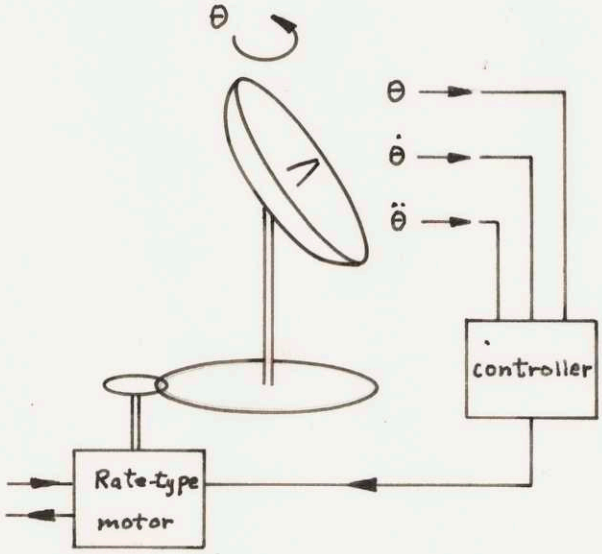

Fig. 3. Azuma Control of Radar Antenna with Fluidic Motor

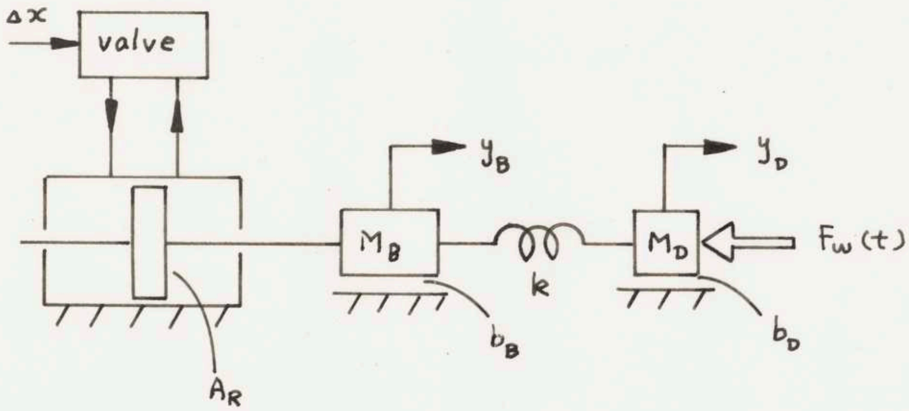

Fig. 4. Idealized Model of Azuma Control of Antenna

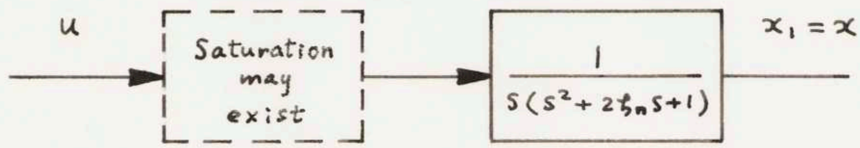

Fig. 5. Normalized Open-loop System

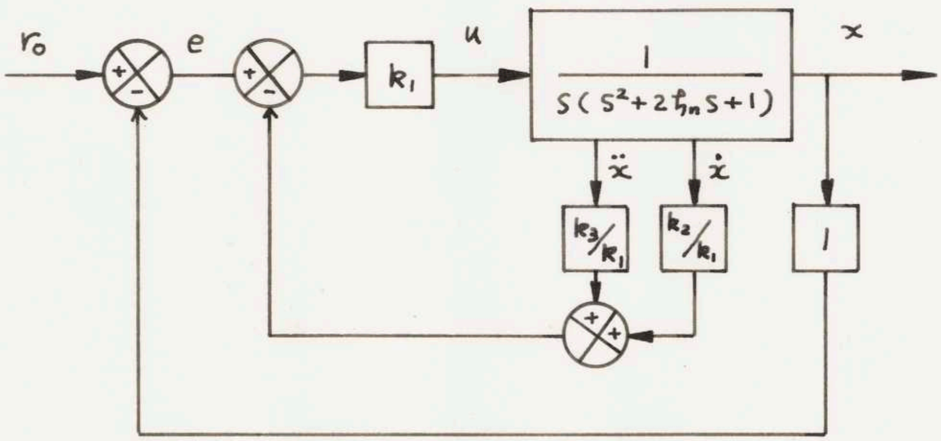

Fig. 6a. Linear Closed-loop System

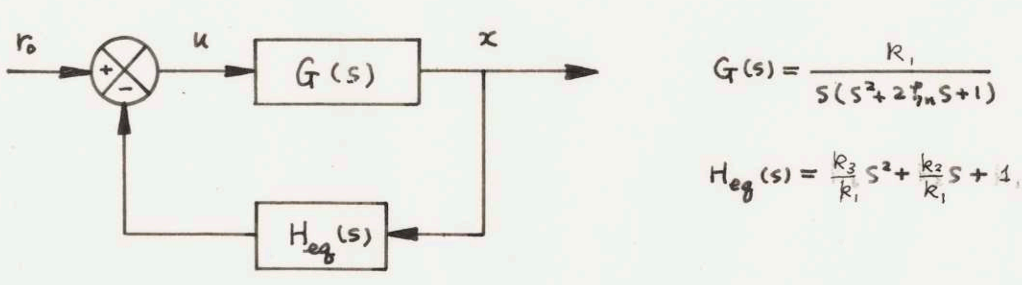

Fig. 6b. Linear Closed-loop System

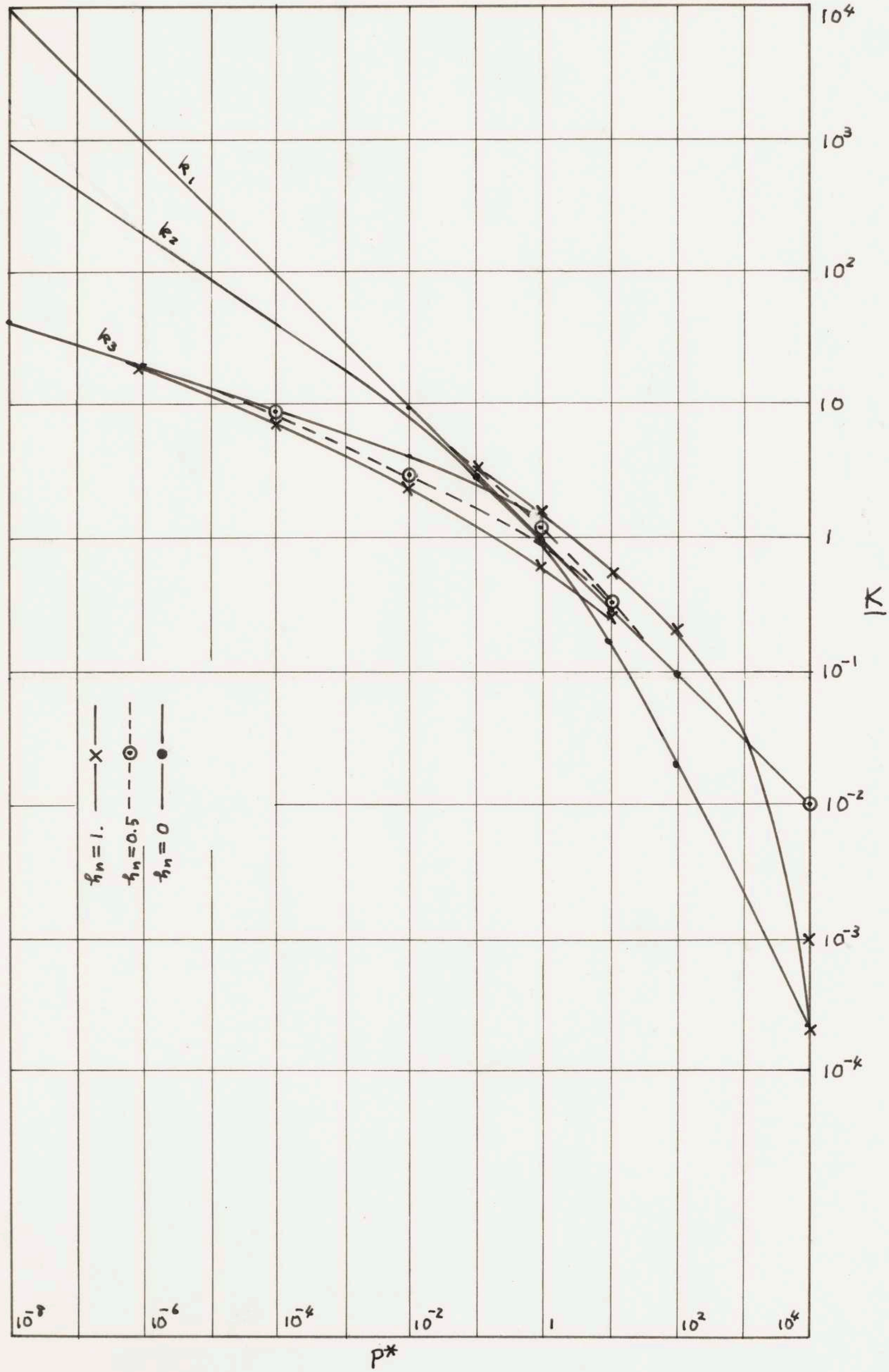

Fig. 7. Optimal Feedback Gains - Weighting Factor in Performance Index

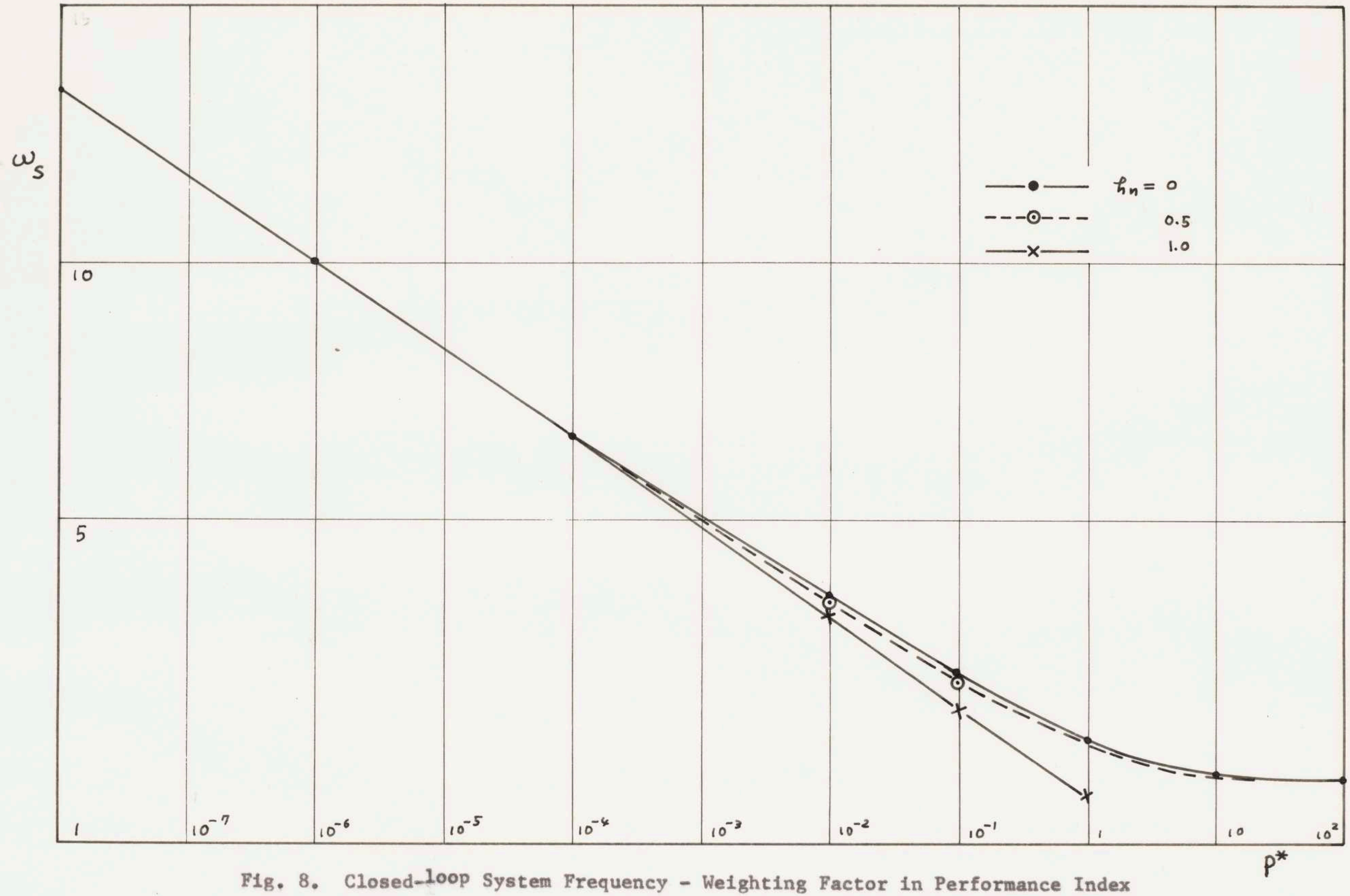

Fig. 8. Closed-loop System Frequency - Weighting Factor in Performance Index

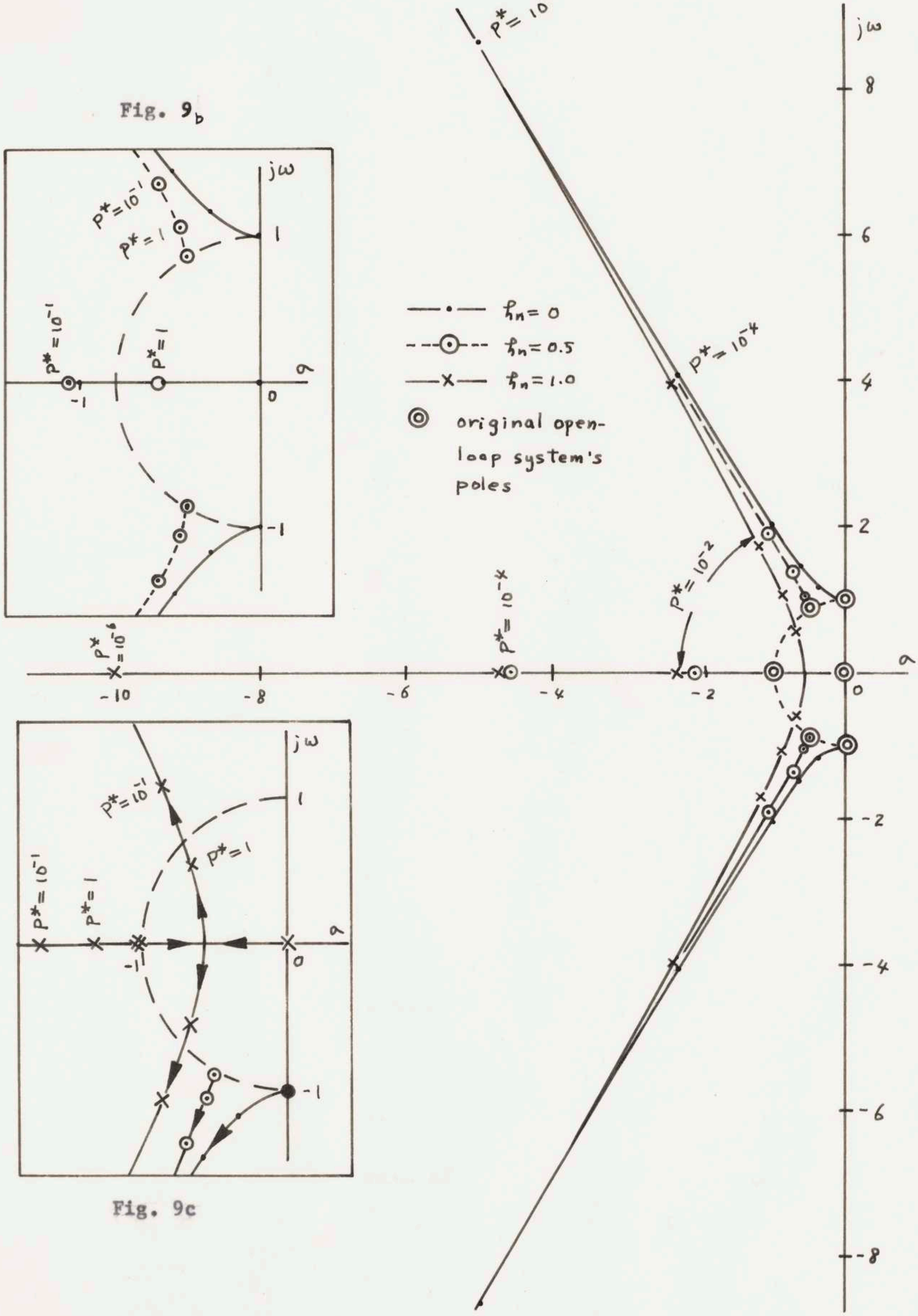

Fig. 9b

Fig. 9c

Fig. 9a. Root Locus of Optimal Closed-loop System

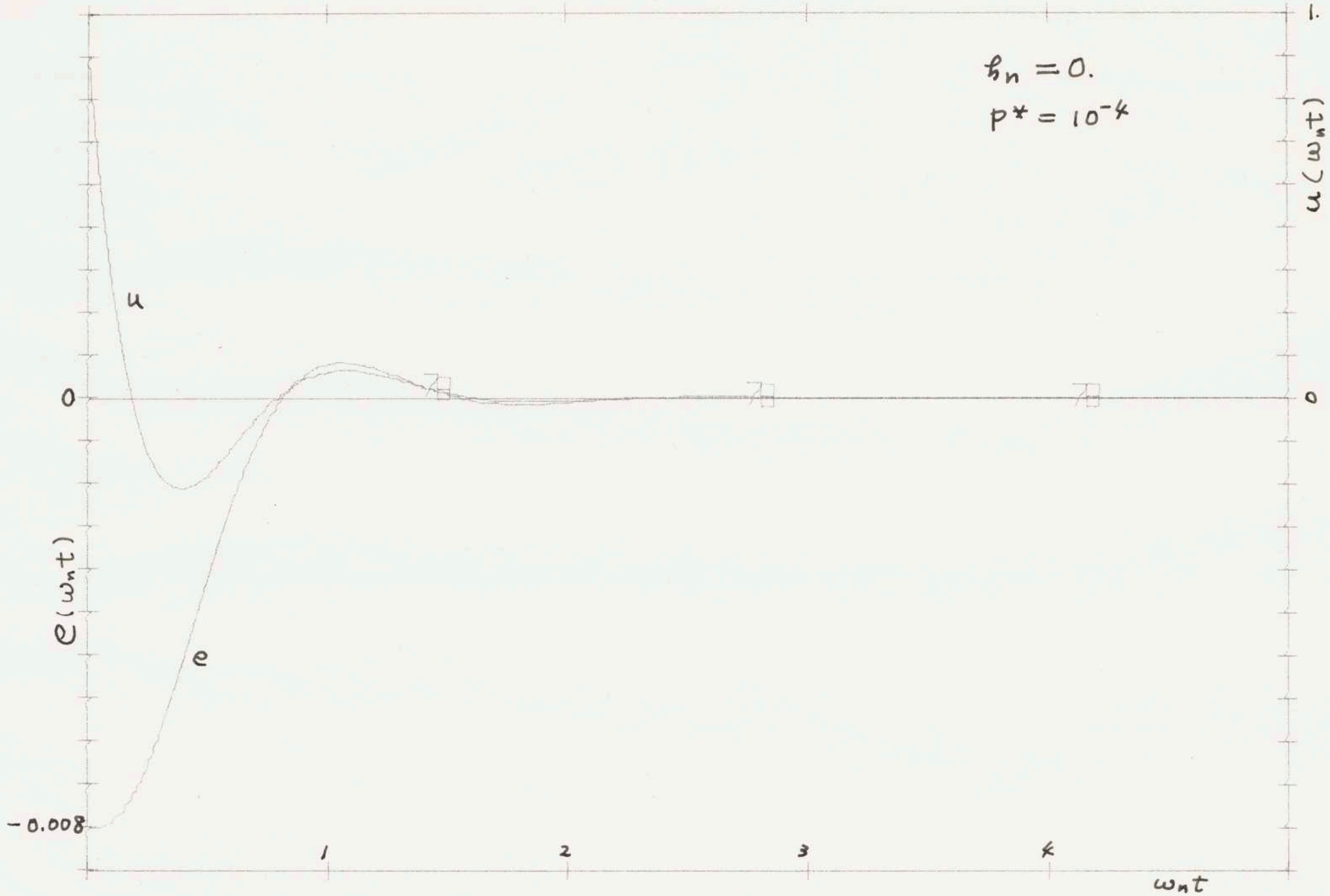

Fig. 10. A Typical Step Response of Linear Optimal Control System

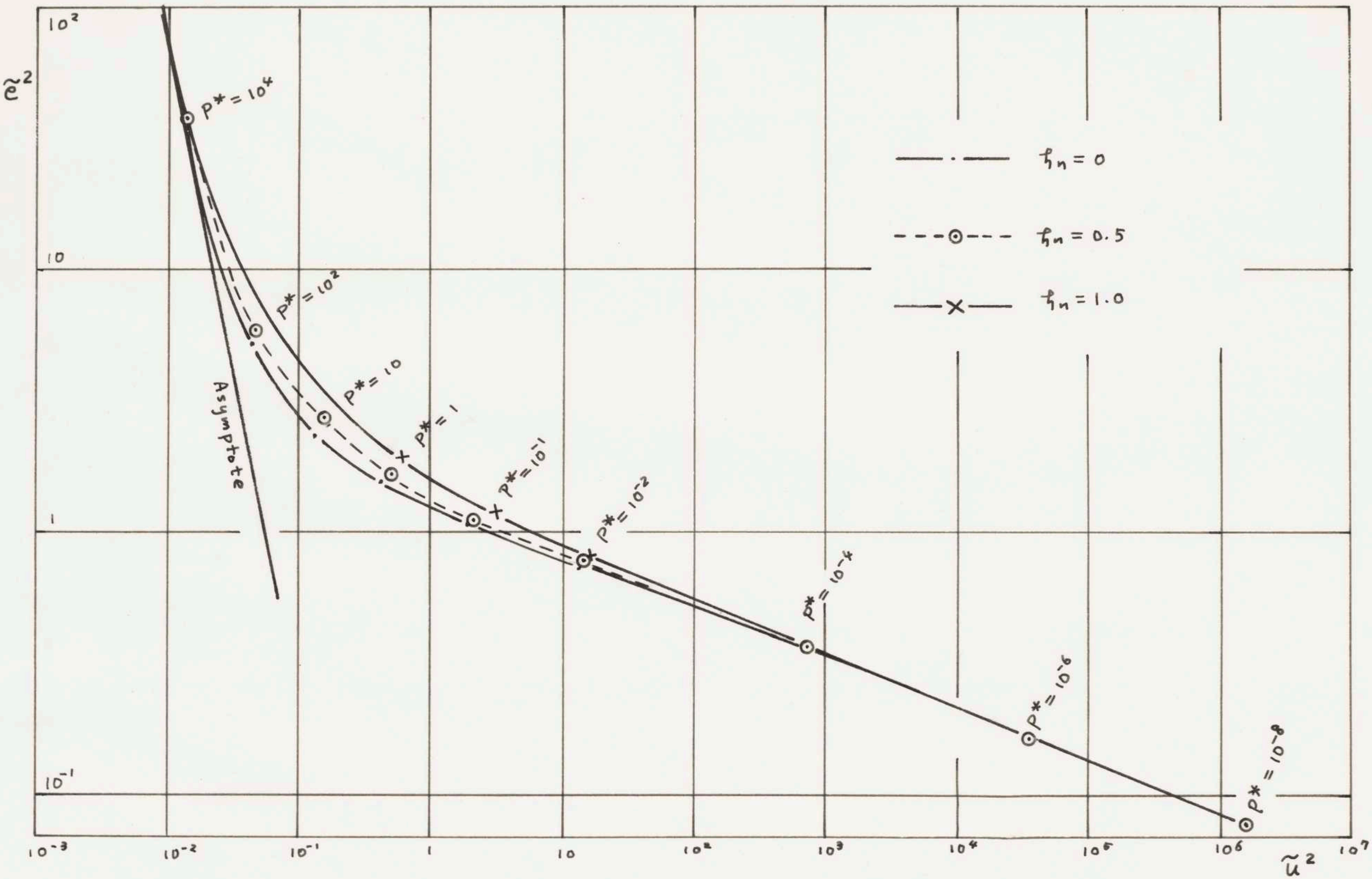

Fig. 11. Evaluation of Performance Index with Linear Optimal Feedback Gains

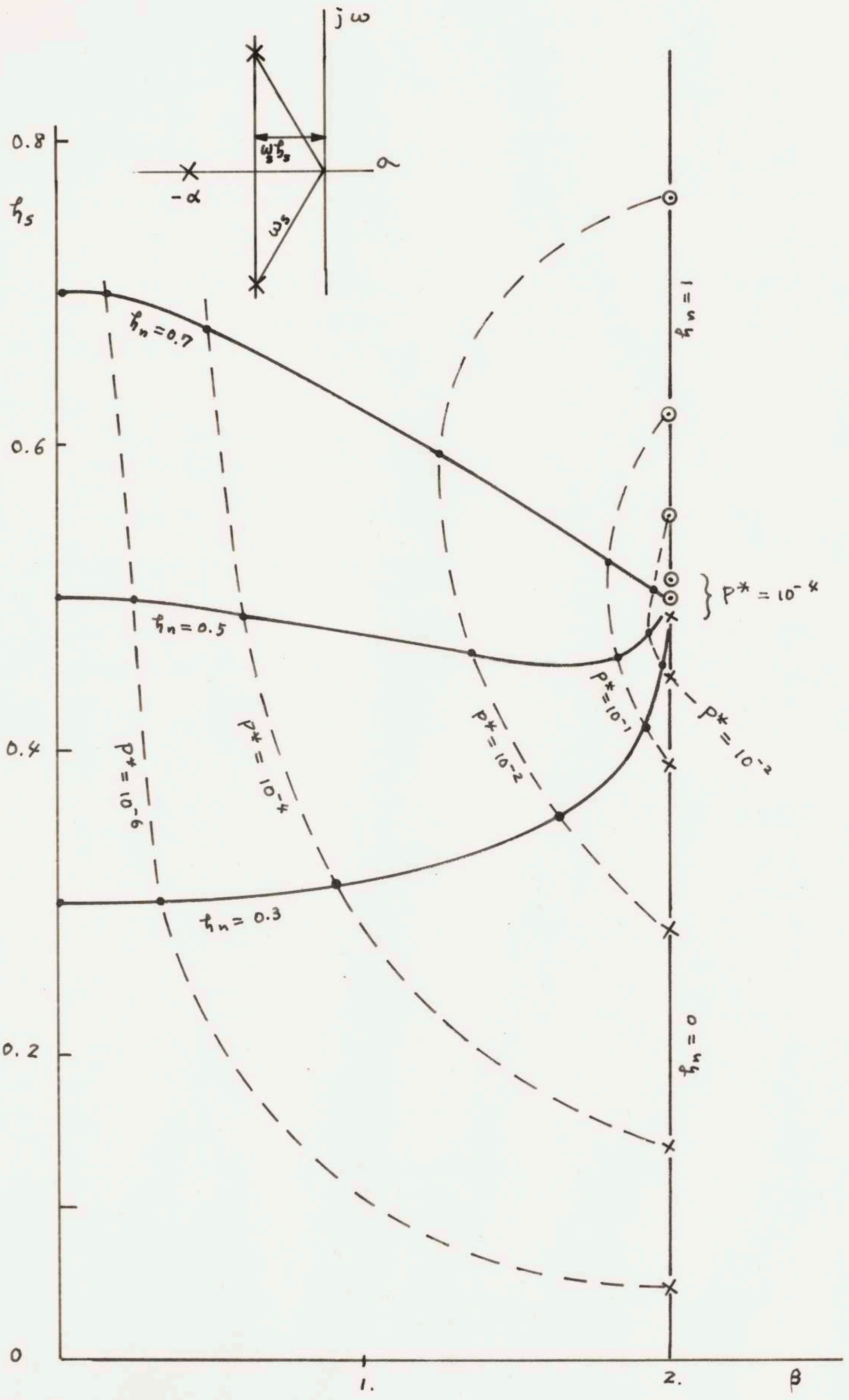

Fig. 12. A Bridge Between Linear Optimal and Conventional Controls

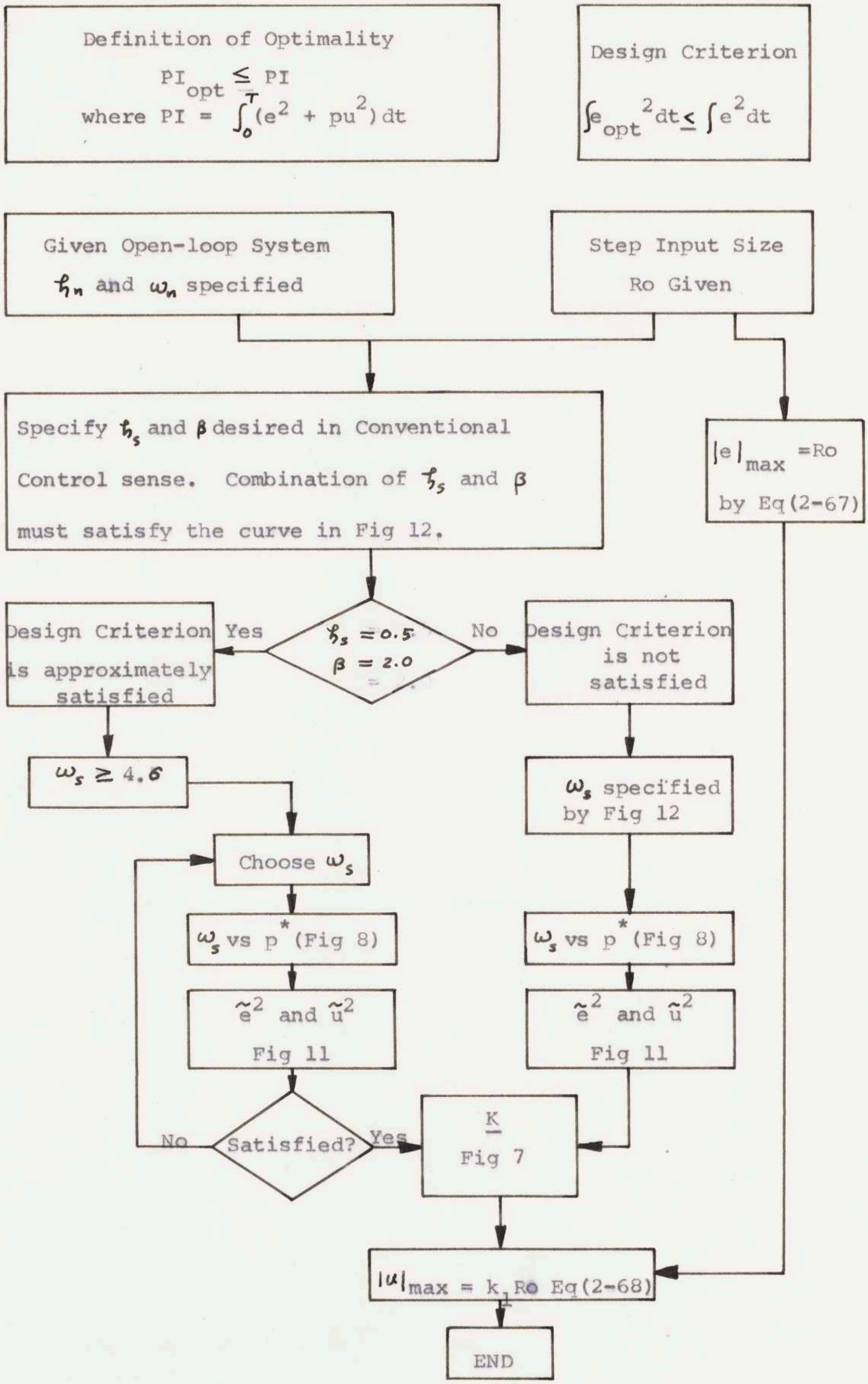

Fig. 13. **Procedure to Find Optimal Control System with Conventional Design Criteria**

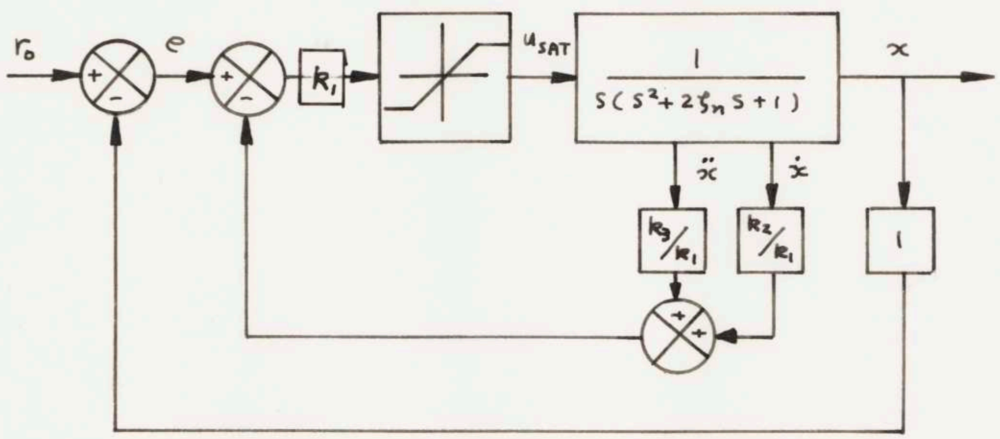

Fig. 14a. Non-linear Closed-loop System

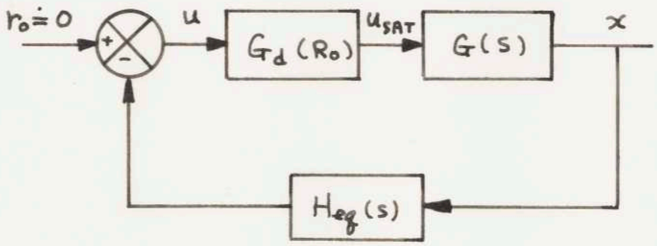

Fig. 14b. Non-linear Closed-loop System

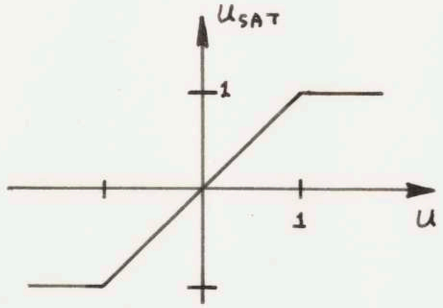

Fig. 15. Characteristics of Saturation

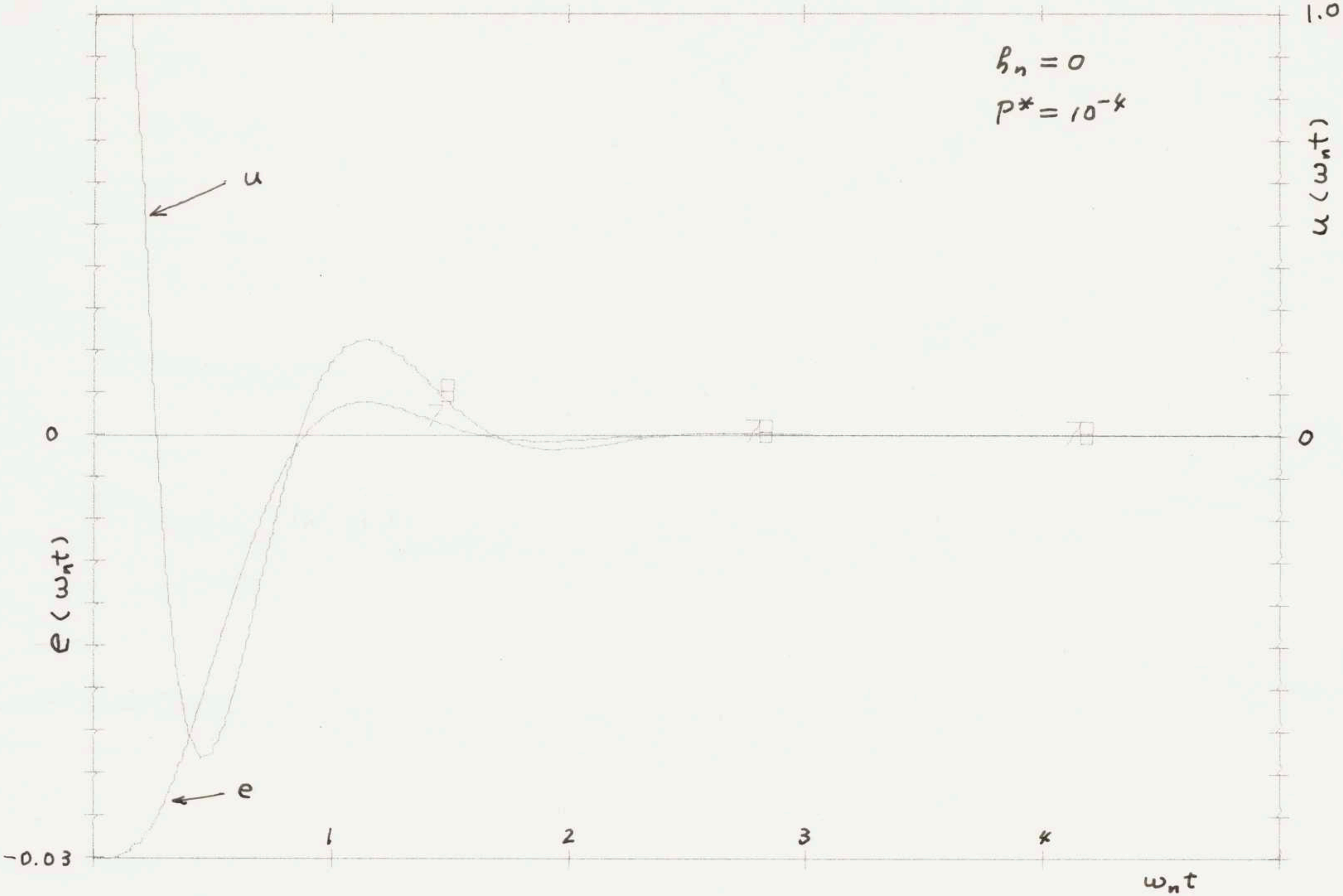

Fig. 16a. A Typical Step Response of Non-linear Control System

Fig. 16b. A Typical Step Response of Non-linear Control System

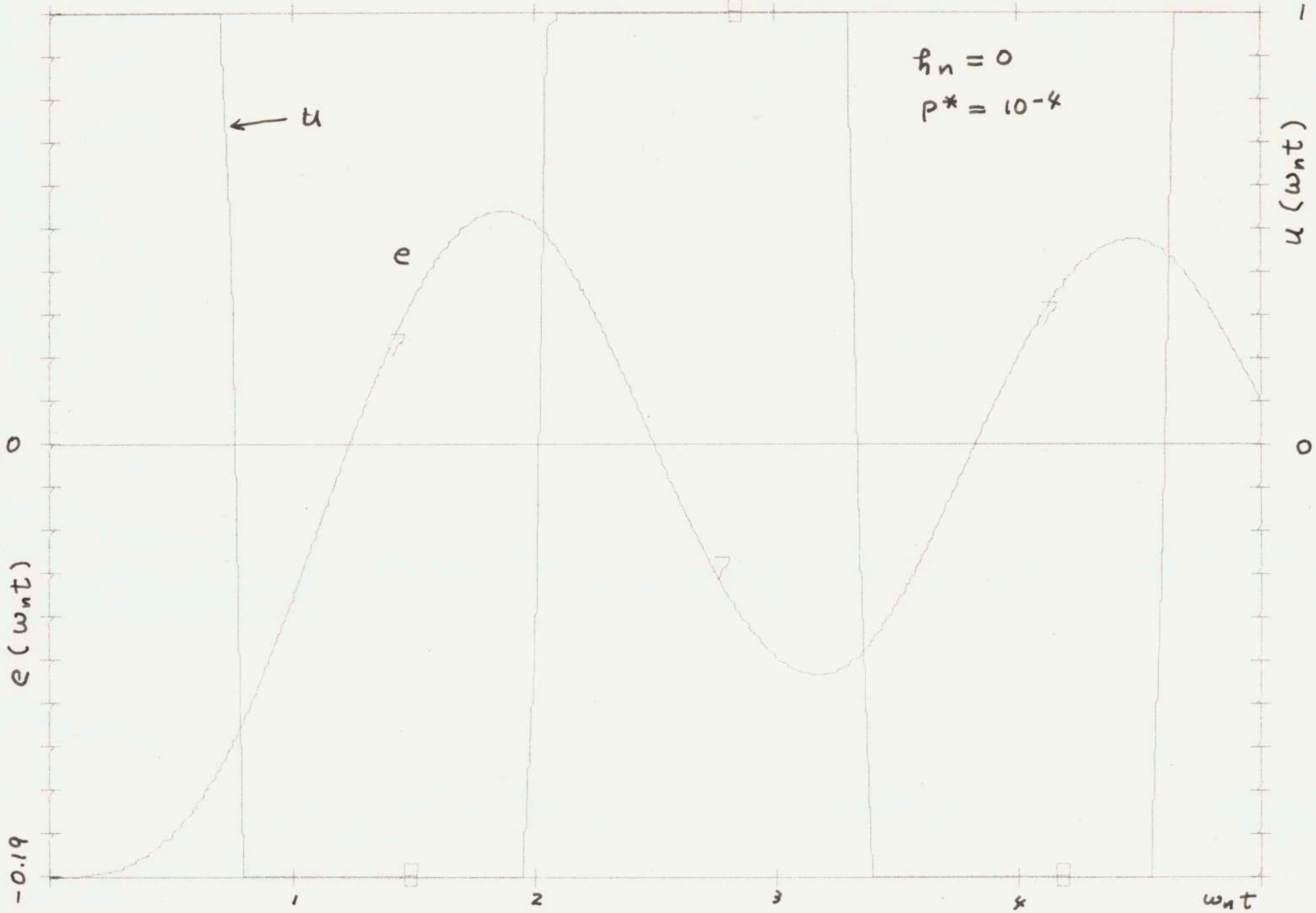

Fig. 16c. A Typical Step Response of Non-linear Control System

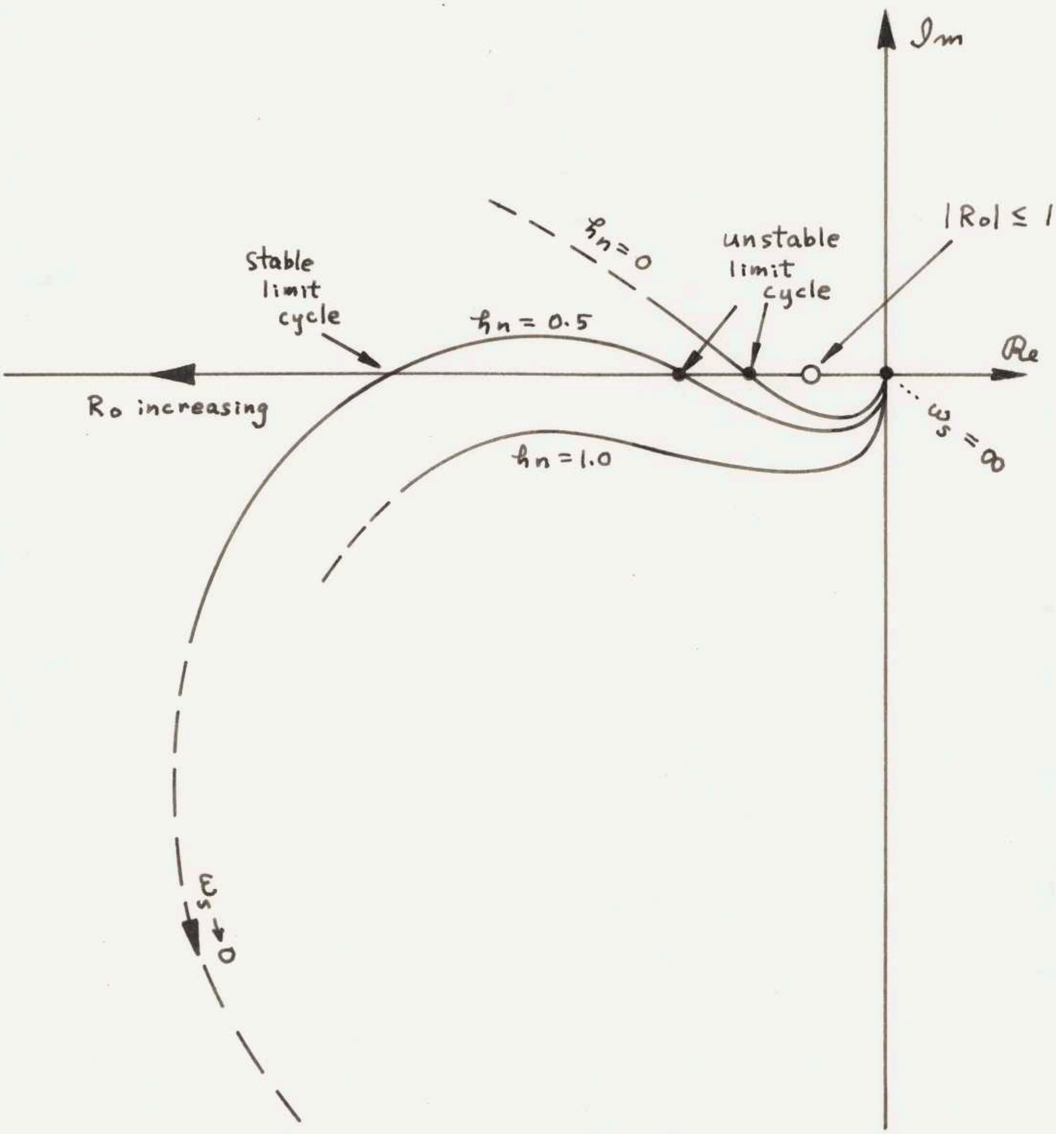

Fig. 17. Nyquist Plot by Using Describing Function

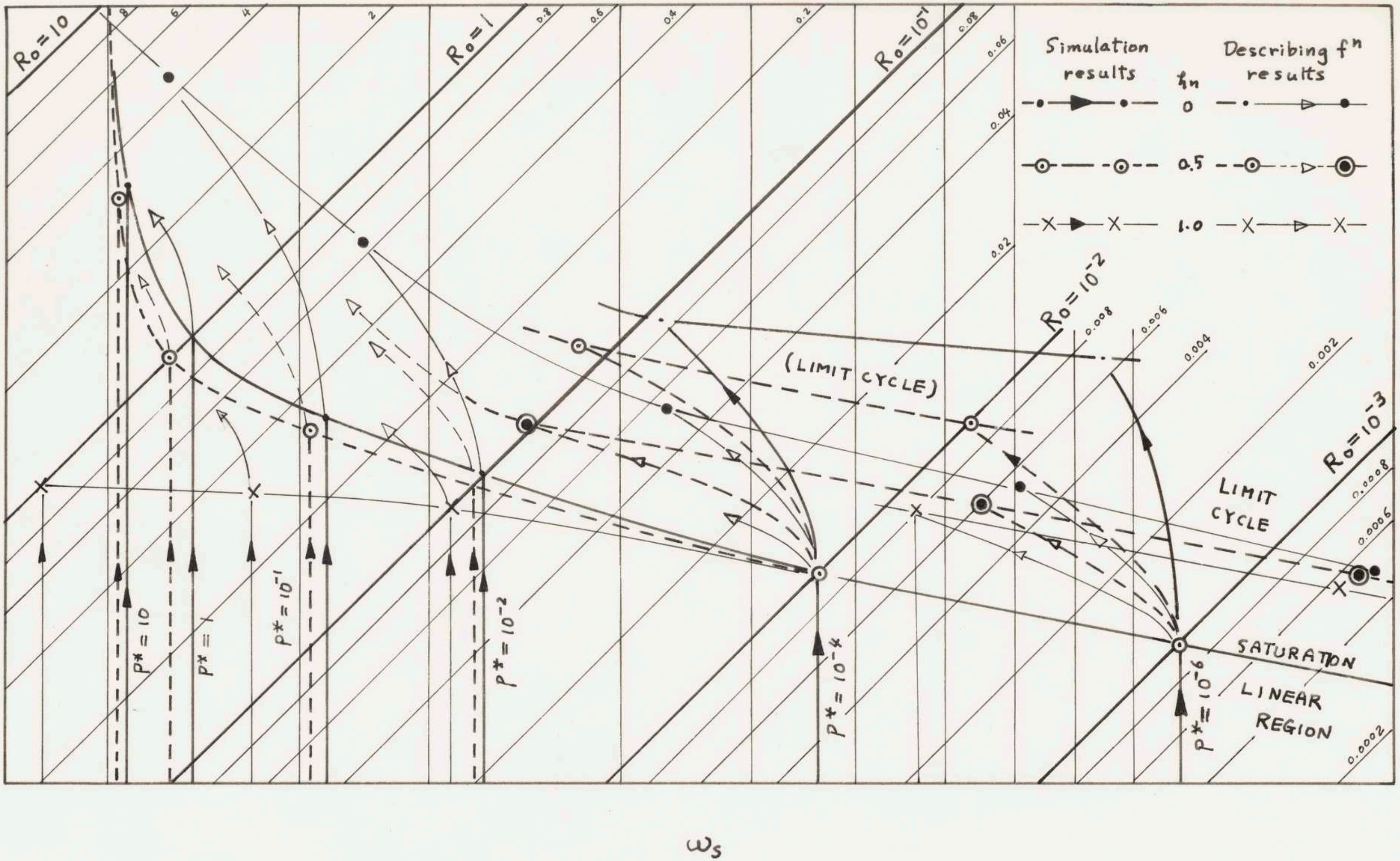

Fig. 18. Effect of Step Input Size on Saturation and Limit Cycle

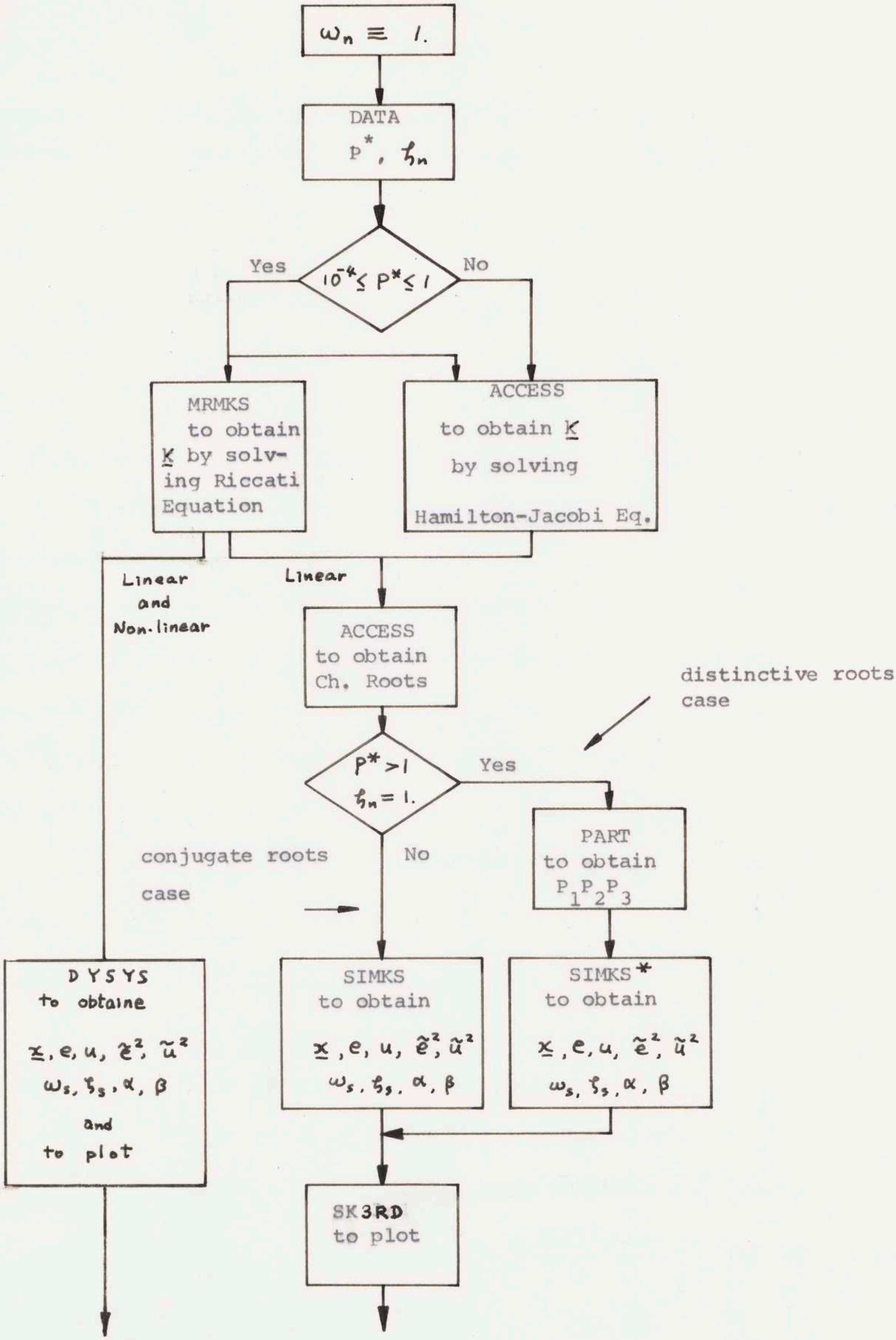

Fig. 19. Computational Procedures

APPENDIX I

Modeling and Formulation of a Saturated Valve-Controlled Rate-type Fluid Motor Connected to a Load-mass through a Spring

(1) Introduction

Analysis of a valve-controlled rate-type fluid motor has been developed [12, 13]. The following analysis is essentially the development for a non-linear case, from the linear case study by Richardson [13]. The valve considered here is open-centered and underlapped. The system configuration is given by Fig. 1a and the valve characteristics by Fig. 1b.

(2) Linearized Dynamic Behavior of a Fluid Motor

The behavior is studied in the vicinity of the steady-state operating points.

Definitions: P_1, P_2 = the pressures of the ram chambers 1 and 2, respectively.

P_s = the supply pressure

Assumption (1): $P_1, P_2 << P_s$ (A-1)

Definitions: u = the valve displacement

u_{max} = the maximum displacement of the valve.

q_{L1} = the flow into the ram-chamber 1

q_{L2} = the flow out of the ram-chamber 2

$\Delta P_1, \Delta P_2, \Delta u, \Delta q_{L1}, \Delta q_{L2}$ = the differential changes in these variables.

$$b_i = \frac{\partial(q_{Li}/q_{max})}{\partial(u/u_{max})} \qquad i = 1, 2 \qquad \text{(A-2)}$$

$$\alpha_i = \frac{\partial (q_{Li} / q_{max})}{\partial (P_i / P_s)} \qquad i = 1, 2 \qquad \text{(A-3)}$$

The linearized valve equations are given by,

$$\frac{\Delta q_{Li}}{q_{max}} = b_i \frac{\Delta u}{u_{max}} + \alpha_i \frac{\Delta P_i}{P_s} \qquad i = 1, 2 \qquad \text{(A-4)}$$

Definitions: $V_{1,2}$ = the volumes of the ram-chambers 1 and 2, respectively.

$V_o = V_{10} = V_{20}$

$= V_{1,2}$ when the ram is at the center position

β = the bulk modulus of the fluid

A_R = the area of the ram

$\Delta\dot{y}_R$ = the differential change in the velocity of the ram

Assumption (2): $$(q_{L1})_{t=0} = (q_{L2})_{t=0} = 0 \qquad \text{(A-5)}$$

The linearized ram-chamber equations are given by,

$$\Delta q_{Li} = \Delta\dot{P}_i \cdot \frac{V_o}{\beta} + A_R \Delta\dot{y}_R \qquad i = 1, 2 \qquad \text{(A-6)}$$

For a symmetrical pair of three-way valves,

$$b_1 = b_2 = b \qquad \text{(A-7)}$$

$$\alpha_1 = \alpha_2 = \alpha \qquad \text{(A-8)}$$

The differential operator is defined by

$$D = \frac{d}{dt} \qquad \text{(A-9)}$$

By substituting for Eq. (A-6) into Eq. (A-4), and subtrututing Eq.'s (A-6) for i = 1 and 2, the linearized valve-ram equation is given by,

$$(\tau_c D + 1)\frac{\Delta P_L}{P_s} = \frac{2b}{\alpha}\cdot\frac{\Delta u}{u_{max}} - \frac{2A_R}{\alpha\, u_{max}} D(\Delta y_R) \qquad \text{(A-10)}$$

where

$$\tau_c = \frac{V_o P_s}{\beta\, u_{max}\, \alpha} \qquad \text{(A-11)}$$

= the time constant of the ram-chambers

$$\Delta P_L = \Delta P_1 - \Delta P_2 \qquad \text{(A-12)}$$

Assumption: the saturation of u, which is given by

$$SAT(\Delta u) = \begin{cases} \Delta u & \text{if } |\Delta u| < u_{max} \\ u_{max} & \text{if } |\Delta u| \geq u_{max} \end{cases} \qquad \text{(A-13)}$$

Eq. (A-9) becomes,

$$(\tau_c D + 1)\frac{\Delta P_L}{P_s} = \frac{2b}{\alpha}\,\frac{SAT(\Delta u)}{u_{max}} - \frac{2A_R}{\alpha\, u_{max}} D(\Delta y_R) \qquad \text{(A-14)}$$

(3) Dynamic Load Characteristics

Definitions: y_R = the position of the ram

y_L = the position of the load-mass

$\ddot{y}_L$ = the accelerations of the load-mass

k = the connection-spring constant

m_L = the load-mass

$F_W(t)$ = the load force on the mass

The load equation connected to the motor is given by

$$(P_1 - P_2)A_R = P_L A_R = k(y_R - y_L) \tag{A-15}$$

and is linearized as,

$$\Delta P_L A_R = k(\Delta y_R - \Delta y_L) \tag{A-16}$$

On the other hand, the dynamics of the load is given by

$$m_L D^2(y_L) + k(y_L - y_R) + F_w(t) = 0 \tag{A-17}$$

Eq. (A-17) is linearized as

$$m_L D^2(\Delta y_L) + k(\Delta y_L - \Delta y_R) + \Delta F_w(t) = 0 \tag{A-18}$$

or

$$\Delta y_R = \frac{1}{k}(m_L D^2 + k)\Delta y_L + \frac{1}{k}\Delta F_w(t) \tag{A-19}$$

From Eq. (A-16) and Eq. (A-18)

$$\Delta P_L = \frac{1}{A_R} m_L D^2(\Delta y_L) + \frac{1}{A_R}\Delta F_w(t) \tag{A-20}$$

(4) Overall Open-loop System Equation

Substituting for Eq.'s (A-19) and (A-20) into Eq. (A-14), the overall system equation with y_L only is given by

$$\left[\left(\frac{\tau_c m_L}{P_s A_R} + \frac{2A_R}{\alpha g_{max}}\cdot\frac{m_L}{k}\right)D^2 + \left(\frac{m_L}{P_s A_R}\right)D + \frac{2A_R}{\alpha g_{max}}\right]D(\Delta y_L)$$
$$= \frac{2b}{\alpha}\cdot\frac{SAT(\Delta u)}{u_{max}} - \left[\left(\frac{\tau_c}{P_s A_R} + \frac{2A_R}{\alpha g_{max}}\frac{1}{k}\right)D + \frac{1}{P_s A_R}\right]\Delta F_w(t) \tag{A-21}$$

which can be written as,

$$\left(\frac{D^2}{\omega_n^2} + \frac{2\zeta_n}{\omega_n}D + 1\right)\Delta\dot{y}_L'$$
$$= k_v' \, SAT(\Delta u') - \left[\left(1 + \frac{k_s}{k}\right)\tau_c D + 1\right]\Delta F_w' \tag{A-22}$$

where the non-dimensionalized constants and variables are defined by,

$$k_s\left(\frac{1}{k}\right) = \frac{2\beta A_R^2}{V_0}\left(\frac{1}{k}\right) = \frac{2 P_s A_R^2}{\tau_c \alpha q_{max}}\left(\frac{1}{k}\right) \qquad \text{(A-23)}$$

$$\frac{1}{\omega_n} = \sqrt{\frac{\tau_c m_L \alpha q_{max}}{2 P_s A_R^2} + \frac{m_L}{k}} = \sqrt{m_L\left(\frac{1}{k_s} + \frac{1}{k}\right)} \qquad \text{(A-24)}$$

$$\zeta_n = \frac{1}{\tau_c}\sqrt{\frac{m_L k}{k_s(k+k_s)}} = \frac{m_L \omega_n}{2 k_s \tau_c} \qquad \text{(A-25)}$$

$$\Delta\dot{y}_L' = \frac{2A_R}{\alpha q_{max}} D(\Delta y_L) \qquad \text{(A-26)}$$

$$k_v' = \frac{2b}{\alpha} \qquad \text{(A-27)}$$

$$\Delta u' = \frac{\Delta u}{u_{max}} \quad \text{and} \quad SAT'(\Delta u') = \begin{cases} \Delta u' & |\Delta u'| < 1 \\ 1 & |\Delta u'| \geq 1 \end{cases} \qquad \text{(A-28)}$$

$$\Delta F_w' = \frac{\Delta F_w}{P_s A_R} \qquad \text{(A-29)}$$

(5) Block Diagram

The block diagram of this system is given by Fig. 2b, with a possible state-variables feedback.

(6) Open-loop System to be Investigated in Thesis

Assumption: $\Delta F_w' = 0$ (A-30)

With this assumption, Eq. (a-22) becomes

$$\left(\frac{D^2}{\omega_n^2} + \frac{2\zeta_n}{\omega_n}D + 1\right)\Delta\dot{y}_L' = k_v' \, SAT(\Delta u') \qquad \text{(A-31)}$$

In order to avoid the complexity on variables, new notations are defined by

$$\dot{y}_L = \Delta\dot{y}_L' \qquad \text{(A-32)}$$

$$u = \Delta u' \quad \text{and} \quad SAT(u) = \begin{cases} u & \text{if } |u| < 1 \\ 1 & \geq 1 \end{cases} \qquad \text{(A-33)}$$

Then Eq. (A-31) becomes

$$\left(\frac{D^2}{\omega_n^2} + \frac{2\zeta_n}{\omega_n} D + 1\right) \dot{y}_L = k_v' \ \mathrm{SAT}(u) \tag{A-34}$$

The input-output relation of the system is given by

$$\dot{y}_L = \frac{k_v'}{\frac{D^2}{\omega_n^2} + \frac{2\zeta_n}{\omega_n} D + 1} \ \mathrm{SAT}(u) \tag{A-35}$$

(7) State-Variables Representation of Open-Loop System

Introducing dimensionless variables,

$$y_L' = \omega_n y_L \tag{A-36}$$

$$\dot{y}_L' = \frac{1}{\omega_n} D(y_L') \tag{A-37}$$

$$\ddot{y}_L' = \frac{1}{\omega_n^2} D^2(y_L') \tag{A-38}$$

Eq. (A-34) can be represented, in dimensionless state-variables form, by

$$D\begin{bmatrix} y_L' \\ \dot{y}_L' \\ \ddot{y}_L' \end{bmatrix} = \begin{bmatrix} 0 & \omega_n & 0 \\ 0 & 0 & \omega_n \\ 0 & -\omega_n & -2\zeta_n\omega_n \end{bmatrix} \begin{bmatrix} y_L' \\ \dot{y}_L' \\ \ddot{y}_L' \end{bmatrix} + \begin{bmatrix} 0 \\ 0 \\ k_v' \end{bmatrix} \mathrm{SAT}(u) \tag{A-39}$$

where $D = \frac{d}{dt}$ as in Eq. (A-9).

Redefining a set of state-variables as,

$$\underline{x} = \begin{bmatrix} x_1 \\ x_2 \\ x_3 \end{bmatrix} = \begin{bmatrix} x \\ \dot{x} \\ \ddot{x} \end{bmatrix} = \begin{bmatrix} y_L' \\ \dot{y}_L' \\ \ddot{y}_L' \end{bmatrix} \tag{A-40}$$

Eq. (A-39) is written as

$$D(\underline{x}) = \begin{bmatrix} 0 & \omega_n & 0 \\ 0 & 0 & \omega_n \\ 0 & -\omega_n & -2\zeta_n\omega_n \end{bmatrix} \underline{x} + \begin{bmatrix} 0 \\ 0 \\ k_v' \end{bmatrix} \mathrm{SAT}(u) \tag{A-41}$$

(8) An Example: Position Control of Radar Antenna

The position control of a radar antenna can be a typical example of this thesis. The schematic diagram of a position control system is shown in Fig. 3a. The Schematic diagram of its idealized model is given by Fig. 4. In order to apply directly the results of this thesis to the example, it is necessary to assume that,

M_B = mass of the base = 0

b_B = friction constant of the base = 0

b_D = friction constant of the antenna with air = 0

F_w = external force on the antenna by wind gust = 0

and A_R includes the gear ratio.

APPENDIX II

Computational Procedures for Analysis

The diagram for the computational procedures is given in Fig. 19. A brief description on each computer program is given below.

MRMKS   This is the modification of MRM [16]. The optimal feedback gains of a linear system defined by

$$\dot{\underline{x}} = \underline{A}\,\underline{x} + \underline{B}\,\underline{u} \tag{A-42}$$

$$PI = \int_0^T (\underline{x}^T \underline{Q}\,\underline{x} + \underline{u}^T \underline{P}\,\underline{u})\, dt \tag{A-43}$$

is obtained by solving the matrix Riccati equation,

$$-\dot{\underline{R}} = \underline{R}\,\underline{A} + \underline{A}^T\underline{R} - \underline{R}\,\underline{B}\,\underline{P}^{-1}\underline{B}^T\underline{R} + \underline{Q} \tag{A-44}$$

for negative time by the forth order Runge-Kutta method.

ACCESE (Phase II)

System ACCESS can handle many kinds of linear matrix operations [17]. For this thesis, ACCESS is used for obtaining the optimal feedback gains for the system defined by Eq. (A-42) and (A-43) by solving the Hamilton-Jacobi equation. ACCESS is also used for finding the eigen values of the $[\underline{A} - \underline{BK}^T]$ matrix of an optimal control system obtained.

PART   For $\zeta_n = 1$ and $P^* \geq 7$, the optimal control system has distinct roots. The step response of the 3rd order system is given by

$$x(t) = 1 + a_1 e^{-P_1 t} + a_2 e^{-P_2 t} + a_3 e^{-P_3 t} \tag{A-45}$$

instead of Eq. (2-37). PART is to obtain these partitioning coefficients a_1, a_2 and a_3.

SIMKS This is the program to simulate the linear optimal control system. ζ_s, ω_s, α, β, $\underline{x}$, e, u, $\tilde{e}^2$, and $\tilde{u}^2$ are obtained and punched out. $\tilde{e}^2$ and $\tilde{u}^2$ are computed by the Simpson's Rule.

SK3RD SK3RD is the program to read the data from the cards punched out by SIMKS and to plot them.

DYSYS After obtaining the optimal feedback gains, DYSYS can simulate the linear or non-linear system concerned by solving up to ten simultaneous 1st-order differential equations by the 4th-order Runge-Kutta method. Plotting is also available. [18]

APPENDIX III

Analytical Evaluations of Asymptotes of the $\tilde{e}^2 - \tilde{u}^2$ Curves

(1) Introduction

$\tilde{e}^2 - \tilde{u}^2$ curve is plotted from the simulation results for the linear control system. Conclusion (5) of the linear analysis shows that this curve approaches one asymptote as P* approaches zero and the other as P* approaches infinity. The following proofs show analytically that these asymptotes are given by

$$\lim_{p^* \to 0} \tilde{e}^2 \cong \frac{5}{3}(3\,\tilde{u}^2)^{-\frac{1}{5}} \tag{A-46}$$

$$\lim_{p^* \to \infty} \tilde{e}^2 \cong \frac{1}{4\,\tilde{u}^2} \qquad \text{for } \zeta_n \neq 0 \tag{A-47}$$

where

$$\tilde{e}^2 = \frac{1}{\omega_s}\int_0^\infty e^2(\omega_s t)\, d(\omega_s t) \tag{A-48}$$

$$\tilde{u}^2 = \frac{1}{\omega_s}\int_0^\infty u^2(\omega_s t)\, d(\omega_s t) \tag{A-49}$$

It should be restated that in the analysis

$$R_o = 1 \tag{A-50}$$

and

$$e(t) = \frac{\omega_s^2 e^{-\alpha t}}{\alpha^2 - 2\zeta_s\omega_s\alpha + \omega_s^2} - \frac{\alpha\, e^{-\zeta_s\omega_s t}\sin(\omega_o t + \psi)}{\sqrt{1-\zeta_s^2}\sqrt{\alpha^2 - 2\zeta_s\omega_s\alpha + \omega_s^2}} \tag{A-51}$$

where

$$\omega_o = \omega_s\sqrt{1-\zeta_s^2}$$

$$\theta = \tan^{-1}\frac{\omega_o}{\alpha - \zeta_s\omega_s}$$

$$\psi = \begin{cases} \tan^{-1}\dfrac{\sqrt{1-\zeta_s^2}}{\zeta_s} - \theta - \pi & \text{if } \theta > 0 \\[2ex] \tan^{-1}\dfrac{\sqrt{1-\zeta_s^2}}{\zeta_s} - \theta & \text{if } \theta \leq 0 \end{cases}$$

and

$$u(t) = k_1 e(t) - k_2 x_2(t) - k_3 x_3(t) \tag{A-52}$$

where

$$x_2(t) = \frac{d}{dt}(-e(t))$$

$$x_3(t) = \frac{d}{dt} x_2(t)$$

Conclusions to be referred to in this Appendix are all made in the linear analysis.

(2) Asymptote as P* approaches zero

Eq. (A-46) is to proved by showing

$$\lim_{P^*\to 0} \tilde{e}^2 \cong \frac{5}{3\,\omega_s} \tag{A-53}$$

$$\lim_{P^*\to 0} \tilde{u}^2 \cong \frac{1}{3}\,\omega_s^5 \tag{A-54}$$

From conclusion (1) of the linear analysis,

$$\lim_{P^*\to 0} \beta = 2. \tag{A-55}$$

$$\lim_{P^*\to 0} \zeta_s = 0.5 \tag{A-56}$$

Therefore,

$$\lim_{P^*\to 0} \alpha = \omega_s \tag{A-57}$$

$$\lim_{P^*\to 0} \frac{\zeta_s}{\sqrt{1-\zeta_s^2}} = \frac{1}{\sqrt{3}} \tag{A-58}$$

$$\lim_{P^*\to 0} \theta = \frac{\pi}{3} \tag{A-59}$$

$$\lim_{P^*\to 0} \psi = -\pi \tag{A-60}$$

For simplicity, let

$$\tau = \omega_s t \tag{A-61}$$

By using Eq. (A-55) through Eq. (A-61),

$$\lim_{p^*\to 0} e^2(\tau) = e^{-2\tau} + \frac{4}{\sqrt{3}} e^{-1.5\tau} \sin\sqrt{0.75}\,\tau + \frac{4}{3} e^{-\tau} \sin^2\sqrt{0.75}\,\tau \tag{A-62}$$

Eq. (A-52) is evaluated as

$$\lim_{p^*\to 0} \tilde{e}^2(\tau) = \frac{1}{\omega_s}\int_0^\infty \lim_{p^*\to 0} e^2(\omega_s t)\, d(\omega_s t)$$

$$= \frac{1}{\omega_s}\,\frac{5}{3}$$

Next, Eq. (A-54) is to be proved. From Conclusion (3)

$$k_1 \cong \omega_s^3 \tag{A-63}$$

$$k_2 \cong 2\omega_s^2 - 1 \tag{A-64}$$

$$k_3 \cong 2\omega_s - 2\zeta_n \tag{A-65}$$

By using Eq's (A-55) through (A-61) and Eq's. (A-63) through (A-65),

$$\begin{aligned} \lim_{p^*\to 0} u^2(\tau) &= e^{-\tau}\left[\omega_s^3 - 2\zeta_n\omega_s^2 + \omega_s\right] \\ &\quad + e^{-0.5\tau}\sin\sqrt{0.75}\,\tau\left[-\frac{2}{\sqrt{3}}\omega_s^3 + \frac{2}{\sqrt{3}}\omega_s^2 + \frac{1}{\sqrt{3}}\omega_s\right] \\ &\quad + e^{-0.5\tau}\cos\sqrt{0.75}\,\tau\left[2\zeta_n\omega_s^2 - \omega_s\right] \end{aligned} \tag{A-66}$$

Therefore $\lim_{p^*\to 0} \tilde{u}^2$ is exactly evaluated as,

$$\begin{aligned} \lim_{p^*\to 0} \tilde{u}^2(\tau) &= \frac{1}{\omega_s}\int_0^\infty \lim_{p^*\to 0} u^2(\omega_s t)\, d(\omega_s t) \\ &= \frac{1}{3}\omega_s^5 + (1-\zeta_n)\omega_s^4 + \left(\frac{1}{6} - \frac{1}{3}\zeta_n + \frac{1}{2}\zeta_n^2\right)\omega_s^3 \\ &\quad + \left(\frac{2}{3} - \frac{5}{3}\zeta_n\right)\omega_s^2 + \frac{1}{3}\omega_s \end{aligned} \tag{A-67}$$

For $P^* < 10^{-4}$, (or $\omega_s > 4.6$), Eq. (A-67) can be approximated by

Eq. (A-54) as

$$\lim_{P^* \to 0} \tilde{u}^2(\tau) \cong \frac{1}{3}\omega_s^5$$

Substituting for Eq. (A-54) into Eq. (A-53), Eq. (A-46) is obtained.

(3) Asymptote as P* approaches infinity ($\zeta_n \neq 0$)

Eq (A-47) is to be proved by showing

$$\lim_{P^* \to \infty} \tilde{e}^2 \cong \frac{1}{2\alpha} \qquad \text{(A-68)}$$

$$\lim_{P^* \to \infty} \tilde{u}^2 \cong \frac{\alpha}{2} \qquad \text{(A-69)}$$

for $0 < \omega_n < 1$.

and

$$\lim_{P^* \to \infty} \tilde{e}^2 \cong \frac{1}{2P_1} \qquad \text{(A-70)}$$

$$\lim_{P^* \to \infty} \tilde{u}^2 \cong \frac{P_1}{2} \qquad \text{(A-71)}$$

for $\omega_n = 1$.

The linear analysis shows that as P* approaches infinity, the control system approaches the original system to be controlled, i.e.,

$$\lim_{P^* \to \infty} \omega_s = \omega_n = 1 \qquad \text{(A-72)}$$

$$\lim_{P^* \to \infty} \alpha = 0^+ \qquad \text{(A-73)}$$

$$\lim_{P^* \to \infty} \zeta_s = \zeta_n \qquad \text{(A-74)}$$

For $0 < \zeta_n < 1$

$\lim_{P^* \to \infty} e^2$ is calculated by applying Eq.'s (A-72) and (A-74) to Eq. (A-51) as

$$\lim_{P^* \to \infty} e^2(t) = (e^{-\alpha t})^2 \tag{A-75}$$

Eq. (A-48) is evaluated as

$$\lim_{P^* \to \infty} \tilde{e}^2 = \frac{1}{2\alpha} \tag{A-76}$$

Generally k_1, k_2 and k_3 are given by

$$k_1 = \alpha \omega_n^2 \tag{A-77}$$

$$k_2 = 2\zeta_n \omega_n \alpha + (\omega_n^2 - 1) \tag{A-78}$$

$$k_3 = \alpha + (2\zeta_n \omega_n - 2\zeta_n) \tag{A-79}$$

As P* approaches infinity, k_1, k_2 and k_3 are approximated by using Eq. (A-72) as

$$k_1 \cong \alpha \tag{A-80}$$

$$k_2 \cong 2\zeta_n \alpha \tag{A-81}$$

$$k_3 \cong \alpha \tag{A-82}$$

Since from Eq. (A-52) $u(\tau)$ is generally given by

$$\begin{aligned} u(\tau) = {} & (k_1 - k_2\alpha + k_3\alpha^2) \frac{e^{-\frac{\alpha}{\omega_s}\tau}}{\alpha^2 - 2\zeta_s \omega_s \alpha + \omega_s^2} \\ & + \left[k_1 - k_2 \zeta_s \omega_s + k_3(\alpha \omega_s^2 - 2\zeta_s \omega_s^2 \alpha)\right] \frac{e^{-\zeta_s \tau} \sin\sqrt{1-\zeta_s^2}\,\tau}{\sqrt{1-\zeta_s^2}\sqrt{\alpha^2 - 2\zeta_s \omega_s \alpha + \omega_s^2}} \\ & + (k_1 - k_3 2\zeta_s \omega_s) \frac{e^{-\zeta_s \tau}}{\sqrt{\alpha^2 - 2\zeta_s \omega_s \alpha + \omega_s^2}} \cos\sqrt{1-\zeta_s^2}\,\tau \end{aligned} \tag{A-83}$$

Eq. (A-49) is evaluated as

$$\lim_{P^* \to \infty} \tilde{u}^2 \cong \frac{1}{2\alpha} \tag{A-84}$$

Substituting for Eq. (A-83) into Eq. (A-76), Eq. (A-47) is obtained.

For $\zeta_n = 1$

As P* approaches infinity, $x_1(t)$ is given by

$$x_1(t) = 1 + a_1 e^{-P_1 t} + a_2 e^{-P_2 t} + a_3 e^{-P_3 t} \tag{A-85}$$

where

P_1, P_2, P_3 = poles of characteristics equation of the control system.

$$a_1 = -\frac{P_2 P_3}{(P_2 - P_1)(P_3 - P_1)} \tag{A-86}$$

$$a_2 = -\frac{P_1 P_3}{(P_1 - P_2)(P_3 - P_2)} \tag{A-87}$$

$$a_3 = -\frac{P_1 P_2}{(P_1 - P_3)(P_2 - P_3)} \tag{A-88}$$

Since

$$\lim_{P^* \to \infty} P_1 = 0 \tag{A-89}$$

$$\lim_{P^* \to \infty} P_2 = 1 \tag{A-90}$$

$$\lim_{P^* \to \infty} P_3 = 1 \tag{A-91}$$

$\lim_{P^* \to \infty} \tilde{e}^2$ is approximately evaluated as

$$\lim_{P^* \to \infty} \tilde{e}^2 \cong \frac{1}{2P_1} \tag{A-92}$$

For the distinct roots case the transfer function of the control system is given by

$$G_c(s) = \frac{P_1 P_2 P_3}{(s + P_1)(s + P_2)(s + P_3)} \tag{A-93}$$

Equating Eq. (A-93) to (2-33) in the linear analysis,

$$k_1 = P_1 P_2 P_3 \quad \text{(A-94)}$$

$$1 + k_2 = P_1 P_2 + P_1 P_3 + P_3 P_2 \quad \text{(A-95)}$$

$$2\zeta_n + k_3 = P_1 + P_2 + P_3 \quad \text{(A-96)}$$

and as P* approaches infinity, by using Eq.'s (A-89) through (A-91),

$$\lim_{P^* \to \infty} k_1 \cong P_1 \quad \text{(A-97)}$$

$$\lim_{P^* \to \infty} k_2 \cong 2P_1 \quad \text{(A-98)}$$

$$\lim_{P^* \to \infty} k_3 \cong P_1 \quad \text{(A-99)}$$

Thus, $\lim_{P^* \to \infty} \tilde{u}^2$ is evaluated as

$$\lim_{P^* \to \infty} \tilde{u}^2 = \frac{P_1}{2} \quad \text{(A-100)}$$

By substituting for Eq. (A-100) into (A-92), Eq. (A-47) is obtained.

REFERENCES

Conventional Control

1. Clark, Robert N., Introduction to Automatic Control, John Wiley and Sons, Inc., 1962, pp. 135, 140-145.

2. Newton, Gould and Kaiser, Analytical Design of Linear Feedback Controls, Wiley Press, 1957, Chapter 9.

Modern Control

3. Schultz and Melsa, State Functions and Linear Control Systems, McGraw-Hill Book Co., 1967, Chapters 7 and 8.

4. Athans and Falb, Optimal Control, McGraw-Hill Book Co., 1966, Chapter 9.

5. Derusso and Roy, State Variables for Engineers, John Wiley and Sons, Inc.

6. Bryson and Ho, Applied Optimal Control, Blaisdell Publishing Co., 1969, pp. 24-41, 108, 240.

7. Kalman, R. E., "When Is A Linear Control System Optimal", Journal of Basic Engineering, 1964.

8. Flügge-Lotz and Titus, "The Optimum Response of Full Third-Order Systems with Contactor Control", Journal of Basic Engineering, 1962.

Non-linear Control

9. Gelb and Vander Velde, Multiple-input Describing Functions and Non-linear System Design, McGraw-Hill, Inc., 1968, pp. 114, 123-124, 523.

10. Gibson, John E., Non-linear Automatic Control, McGraw-Hill Book Co., Inc., 1963, pp. 357, 364.

11. Garg, Devendra P., "A Computer-oriented, Parameter-space Approach to the Synthesis of Non-linear Control Systems", Joint Automatic Control Conference, 1970.

Fluid Power Control

12. Blackburn, Reethof and Shearer, Fluid Power Control, The M.I.T. Press, 1960, Chapters 4, 15, and 17.

13. Richardson, Herbert H., "The Analytical Design of Valve-controlled Hydraulic Power and Control Systems: A Case Study", M.I.T., 1962, pp. 14-01 through 14-66.

14. Meyfarth, Philip F., "Analitical Comparison of the Linear and Bang-bang Control of Pneumatic Servomechanisms", S.M. Thesis at M.I.T., 1958.

15. Meyfarth, Philip F., "Dynamic Response Plots and Design Charts for Third-Order Linear Systems", Research Memorandum No. R. M. 7401-3, M.I.T., 1958.

Computer Softwares

16. Sidell, Richard S. "MRM", M.I.T. M. E. Dept. Computer Room, 1969.

17. Sidell, Richard S., "ACCESS (Phase II)", M.I.T. M.E. Dept. Computer Room, 1969.

18. Sidell, Richard S., "DYSYS", M.I.T., M.E. Dept. Computer Room, 1969.